To the Graduate Council:

I am submitting herewith a thesis written by Anne M. Kroman entitled "Backward and Forward: The Gurdjian Theory and Blunt Force Impact of the Human Skull." I have examined the final paper copy of this thesis for form and content and recommend that it be accepted in partial fulfillment of the requirements for the degree of Master of Arts, with a major in Anthropology

Murray K. Marks, Major Professor

We have read this thesis and recommend its acceptance:

Acceptance for the Council:

Vice Provost and Dean of Graduate Studies

Thesis
2003
.K88

Backward and Forward: The Gurdjian Theory and Blunt Force Impact of the Human Skull

A Thesis
Presented for
Master of Arts
Degree
University of Tennessee, Knoxville

Anne M. Kroman
August 2003

Dedication

I would like to dedicate this thesis to my parents, Jim and Deb Kroman.
With out their constant love and support I would not be where I am today.

Acknowledgements

I would like to offer a sincere thank you to all the members of my committee, Drs. Marks, Klippel, and Bass. With out their support and help, this would not be possible. All three have been kind, helpful, and encouraging. Dr. Murray Marks, as my major professor and chair, has provided unending support during my time here at UT for which I am greatly indebted.

I would also like to thank a few other people who were crucial to this project. Dr. Tyler Kress was a wonderful help and provided the means to get this project started. I could not have done it with out him. Also, to Dr. Stephan Duma and the entire staff of graduate students at the Virginia Tech Impact Biomechanics, thank you for your generous gift of time and space. Thank you to Hollee Taylor for her support and assistance during testing.

Thank you to Dr. Steven Symes, Dr. Hugh Berryman, and Dr. O.C. Smith for valuable insight into the project and its applications. I would also like the thank Dr. Symes and Dr. Ran Donaldson for countless hours of proof reading and wonderful suggestions. I am very grateful to the both of you.

My friends and family deserve great thanks as well for providing wonderful emotional support as well as proof reading. A special thanks to

Liz DiGangi and Mariateresa Tersigni for all of their help and for listening to me vent. Thank you to the staff of the National Forensic Academy, for encouragement and compassion in understanding why I was so stressed most of the time.

Abstract

Even though trauma to bone has been an area of keen interest in medicine for decades, forensic anthropology's treatment of blunt force trauma is a fairly new area of research. Correct fracture pattern analysis can provide information concerning number, direction, and order of blows (Berryman and Symes 1999). E.S. Gurdjian (1945, 1947, 1950a, 1950b) conducted a number of studies on blunt force fracture propagation that are still heavily used today.

Gurdjian proposed that applying a brittle substance known as "stresscoat" to the cranial bone surface would replicate impact stresses. Using stresscoat research, Gurdjian characterized blunt force trauma fracture patterns for the skull. Fractures were noted to initiate in an area other than the point of impact, radiating towards it. The fields of forensic anthropology and pathology rely heavily on the predictions made by Gurdjian et al and commonly cite this research in the literature. In fracture patterns interpretation, Gurdjian's results are often used to suggest that the point of impact is at a location other than the fracture epicenter.

This study is a systematic examination and retesting of the theories of fracture propagation as set forth by ES Gurdjian and colleagues using

current biomechanics research and technology. Specifically, the relationship of impact site and fracture patterning was tested using five cadaver heads. The results from all five tests show that fractures radiate directly from the point of impact. In conclusion, the fracture pattern predictions made by Gurdjian and colleagues from the stresscoat results can not be extrapolated to fresh cadaveric bone.

Table of Contents

Chapter 1: Introduction and statement of purpose 1

Chapter 2: Basic biomechanical properties and measurements of human bone 4

Chapter 3: The theories of E.S. Gurdjian and colleagues 21

Chapter 4: Materials and methods 34

Chapter 5: Results 44

Chapter 6: Discussion 62

References 67

Vita 73

List of Figures

Figure 2.1	Illustration of the effect of tensile, compressive, and shear stress on a beam.	7
Figure 2.2	Stages of elastic deformation of bone.	9
Figure 2.3	Stages of plastic deformation of bone.	9
Figure 2.4	Structure and microstructure of human femur.	12
Figure 2.5	Anisotropic materials.	13
Figure 2.6	Diagram showing a typical stress-strain curve showing the elastic and plastic deformation phases and failure point.	15
Figure 2.7	The absorbed energy before failure is calculated by the total area under the curve.	16
Figure 2.8	Fracture propagation in both the inner and outer tables of the cranium.	18
Figure 2.9	Concentric and Radiating fractures from blunt force trauma impact site to the left parietal (10X).	19
Figure 3.1	Views of Macaque skull after impact with the cracks in the stresscoat highlighted with India ink.	22
Figure 3.2	The areas of inbending and outbending associated with impact site.	27
Figure 3.3	Left lateral view of the skull demonstrating the inbending and outbending that occurs from blunt impact.	32
Figure 3.4	An illustration of the "struck hoop" analogy that Knight adapated from Gurdjian.	33
Figure 4.1	Set up of a standard drop tower structure.	36

Figure 4.2	Location of load cells.	37
Figure 4.3	Impact area on left parietal with intact soft tissue, and clean bone on the rest of the cranium in a head ready for testing.	39
Figure 4.4	The skull positioning in the drop tower with overlap height.	41
Figure 5.1	Fracture pattern in test one in the left parietal, with impact site 2 in (5.08 cm) from sagittal suture .6 in (1.52 cm) from coronal suture, and 2.5 in (6.35 cm) from the sqaumosal suture.	45
Figure 5.2	Force in pounds (recorded in scientific notation) to time in milliseconds for Test 1.	46
Figure 5.3	Fracture pattern in the left parietal for test two with an impact site 2 in (5.08 cm) from the sagittal suture, .75 in (1.91 cm) from the coronal suture, and 2 in (5.08 cm) from the sqaumosal suture.	48
Figure 5.4	Force in pounds (recorded in scientific notation) to time in milliseconds for Test 2.	49
Figure 5.5	Fracture pattern in test three in the right parietal, with impact site 2 in (5.08 cm) from sagittal suture .75 in (1.91 cm) from coronal suture, and 3.5 in (8.89 cm) from the sqaumosal suture.	51
Figure 5.6	Force in pounds (recorded in scientific notation) to time in milliseconds for Test 3.	52
Figure 5.7	Force in pounds (recorded in scientific notation) to time in milliseconds for Test 4.	54
Figure 5.8	Fracture pattern in test three in the right parietal, with impact site 2.5 in (6.35 cm) from sagittal suture .75 in (1.91 cm) from coronal suture, and 3.5 in (8.89 cm) from the sqaumosal suture. Extensive fracture are present at the area of impact.	56

Figure 5.9 Right parietal, area on the opposite side from impact. 57

Figure 5.10 The frontal view of the skull used in test five and resulting fractures. There were bilateral fracture of both fronto-zygomatic sutures (insert). 58

Figure 5.11 Force in pounds (recorded in scientific notation) to time in milliseconds for Test 5. 59

Figure 5.12 The line of fracture propagation (read left to right) in test five. 61

Chapter 1: Introduction and statement of purpose

Fracture pattern recognition and interpretation are essential to forensic anthropology. In many cases, accurate interpretation of fractures may be the only objective means of determining cause and manner of death (Berryman and Symes 1998, LeCount and Apfelback 1920). In postmortem trauma assessment the accurate fracture interpretation is essential for identifying the location of impact sites, sequencing blows, and establishing the characteristics of the object responsible for injury (Berryman and Symes 1998). One major area of trauma analysis is blunt force trauma interpretation. The cranium is the region most commonly affected by blunt force trauma and cranial injuries are some of the most complicated to understand (Mortiz 1954). Cranial trauma analysis provides information crucial to establishing the mechanism of death. Cranial fracture interpretation provides information regarding the number of blows to the head, exact location of impact, and size or type of object used to inflict the destructive force (Mortiz 1954).

While the analysis of fracture patterns is an important part of forensic anthropology, most current research and knowledge is taken from forensic specimens that are examined for trauma analysis in a postmortem setting. While this type of research is crucial to the field, it is always after

the fact. The study of blunt trauma is difficult due to the fact that "studies refer to very brief and unforeseeable phenomena whose consequences endanger the health and life of subjects previously in perfect health" (Chapon 1984). The fields of forensic anthropology and trauma research afford little opportunity to study fracture patterning in a controlled experimental setting. Because this research is lacking, there is much speculation about fracture interpretation, as well as reliance on older outdated studies.

One of the key researchers to contribute to area of blunt force trauma interpretation was E.S. Gurdjian. Gurdjian and colleagues conducted research on cranial fractures, and extensively published on the topic. Today his work is still considered the golden standard for the field.

The objective of this study is to evaluate the research done by Gurdjian and coworkers (1945, 1947, 1950a, 1950b) who demonstrated how the cranial vault responds to blunt impact. The theories of Gurdjian state that fracture initiation in the parietal begins at a location other than the impact site and radiates back towards it (1947, 1950a, 1950b). Gurdjian's studies were the height of innovation and advancement at the time, but with the wealth of new technology in impact biomechanics, it is important to retest and evaluate. His theories will be examined and tested utilizing a

drop tower system to simulate a blunt trauma impact. A load cell will measure all forces in millisecond intervals. Fracture propagation will be captured using high-speed video. By filming at a speed faster than the fracture can travel through bone, it will allow the entire fracture event to be viewed and analyzed while it is happening. The resulting data will be compared to results from the Gurdjian et al studies and known blunt trauma forensic cases.

Chapter 2: Basic biomechanical properties and measurements of human bone

Biomechanics is the application of the physical science of forces and energies to living tissue. The application of biomechanics to skeletal material is necessary to understand bone fractures in a rational context. An understanding of biomechanics and the physical properties of bone lends valuable insight into the mechanics of fracture creation and propagation. The creation of fractures is dependent on several factors. First, there are the three extrinsic factors of an applied load type, magnitude, and the rate of application (Gonza 1982). Second, intrinsic characteristics of bone influence the creation and propagation of fractures, including both the material and structural properties (Gonza 1982).

Definitions and Basic Principles of Biomechanics

To understand how bone responds to forces, and how fractures occur, it is important to understand the basic physics terminology of biomechanics. Some basic definitions of important concepts follow. For further review see Brinckmann et al (2002), Cowin (1989), Evans (1970), Frost (1967), Low and Reed (1996), and Roark and Young (1975)

Force

The impacting force or load type plays an important role in fracture creation and propagation. Force is defined as an "action or influence" that is "applied to a free body" (Turner and Burr 1993: 595). In other words, a force is anything that alters the state of motion of an object (Low and Reed 1996). A force simply pushes or pulls on an object. Newton's first law of motion states that a force must be applied to change the velocity or direction of movement of an object. Newton's second law of motion states that the resulting change in momentum of the object is proportional to the force applied (Low and Reed 1996). As an example, the more force that is applied in hitting a baseball with a bat, the faster the ball will travel. Force (F) is calculated as mass (m) times acceleration (a).

$$F = ma$$

Force is measured in newtons (N) or pounds (lbs). Force is a "vector quantity," meaning that it has direction o a magnitude. This is important to trauma biomechanics, where the direction of the force to the bone is very important as explained later.

Load

A load is a force, or combination of forces that is sustained by an object (Frost 1967, Low and Reed 1996). For example, the weight of the body on the foot is a load.

Stress

When examining load type, the most common terminology used is "stress." Stress is defined as "force per unit area" (Turner and Burr 1993: 595), thus calculated:

$$Stress = force/area$$

Stress is calculated by newtons per square meter. The unit of 1 newton per square meter (Nm^{-2}) is 1 pascal. Stress is reported in pascals.

Stress is further subdivided into the three areas: compressive, tensile, and shear (Figure 2.1) (Alms 1961, Turner and Burr 1993, Nordin and Frankel 1980). Compressive stress is developed when a load acts to make the material shorter. Likewise, tensile stress is formed when load works to stretch the material. Shear stress results when one area of material slides into another area. These three types of stress do not exist in isolation. No matter how simple the loading scheme, compressive, tensile, and shear stress are always occurring in combination.

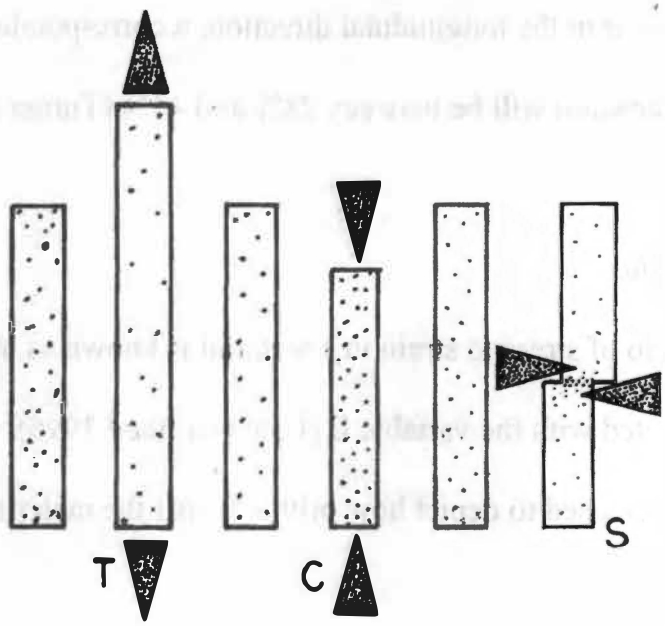

Figure 2.1 Illustration of the effect of tensile (T), compressive (C), and shear (S) stress on a beam. (After Frost 1967: 10).

Strain

The magnitude of load is referred to in terms of strain. Strain is defined as "percentage change in length, or relative deformation" (Turner and Burr 1993).

Strain = increased length/ original length

Since strain is ratio derived, there are no units of measure strain.

Poisson's ratio

Poisson's ratio describes the ratio of change due to strain in length and width (Turner and Burr 1993). Ashman et al (1984) reports a range in Poisson's ratio between .28 and .45. To summarize, if 1% strain is applied

to a human femur in the longitudinal direction, a corresponding strain in the horizontal dimension will be between 28% and 45% (Turner and Burr 1993).

Young's modulus

The ratio of stress to strain in a material is known as Young's modulus, denoted with the variable E (Low and Reed 1996). Young's modulus is often used to depict how brittle or stiff the material is.

Deformation

Materials under stress pass through two many stages before failure. These are elastic and plastic deformation (Low and Reed 1996). Elastic deformation is a state when a material can return to its original form, once pressure is released (Figure 2.2). An example of elastic deformation sponge that changes shapes when squeezed then returns to its original form when released. Plastic deformation is a level of deformation from which the material will never recover (Figure 2.3). An example is a paper clip, once unfolded it will never be exactly the same.

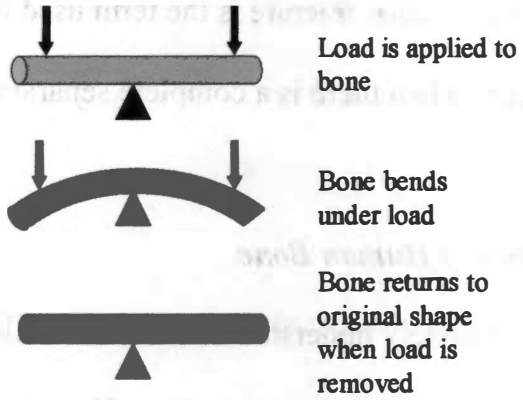

Figure 2.2 Stages of elastic deformation of bone.

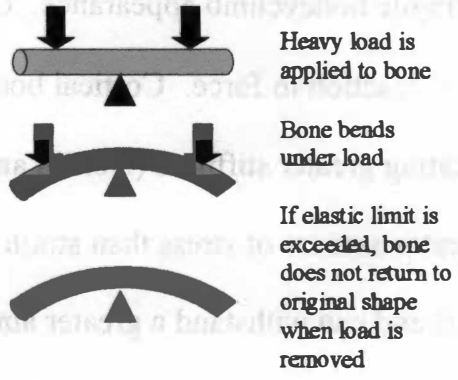

Figure 2.3 Stages of plastic deformation of bone.

Fracture

In bone trauma, fracture is the term used for failure of bone. A fracture occurs when there is a complete separation of molecules (Low and Reed 1996).

Biomechanics of Human Bone

To completely understand bone trauma biomechanics, it is just as important to understand the properties of bone as a tissue as it is to understand basic biomechanics.

Bone Tissue Structure

Vertebrate skeletal systems contain two types of bone, cortical or compact and cancellous or spongy (Harkess et al 1984). Cortical bone is stiff and more dense while cancellous bone is porous and lightweight with a characteristic fragile honeycomb appearance. Cortical and cancellous bone differs greatly in reaction to force. Cortical bone has a higher Young's modulus, indicating greater stiffness (Nordin and Frankel 1980). It can withstand a greater amount of stress than strain before failure. Cancellous bone is less stiff and can withstand a greater amount of strain than cortical bone. Cortical bone fails when strain exceeds 2%, while cancellous bone can withstand up to 7% (Nordin and Frankel 1980: 21).

Bone Histology

Bone is composed of cells and an extracellular matrix. The cells of the bone include osteoblasts, osteoclasts, and osteocytes (Bouvier 1989). Osteoblasts are cuboidal cells which are responsible for the secretion of bone matrix. Osteoclasts are larger, multinucleated cells responsible for the absorption of bone. Osteocytes are osteoblasts that are trapped with in the bone, and responsible for maintenance. These circular structures that house the osteocytes are known as osteons (Figure 2.4).

Material Properties of Bone

Both cortical and cancellous bones are anisotropic materials (for review see Antich 1993, Bonfield et al 1985, Evans 1973, Johnson 1985, Keaveny and Hayes 1993, Nordin and Frankel 1980, Turner and Burr 1993). Characteristically, anisotropic materials have different material properties based on direction (Figure 2.5). This differs from isotropic materials which are more homogenous having the same material properties in all directions. Human cortical bone has a particular type of anisotropy referred to as transverse isotropy, because it has the same resistance to force in all transverse directions, and a higher resistance in the longitudinal direction (Keaveny and Hayes 1993). The histology of bone contributes to its anisotropy. Human bone is stronger in the longitudinal dimension

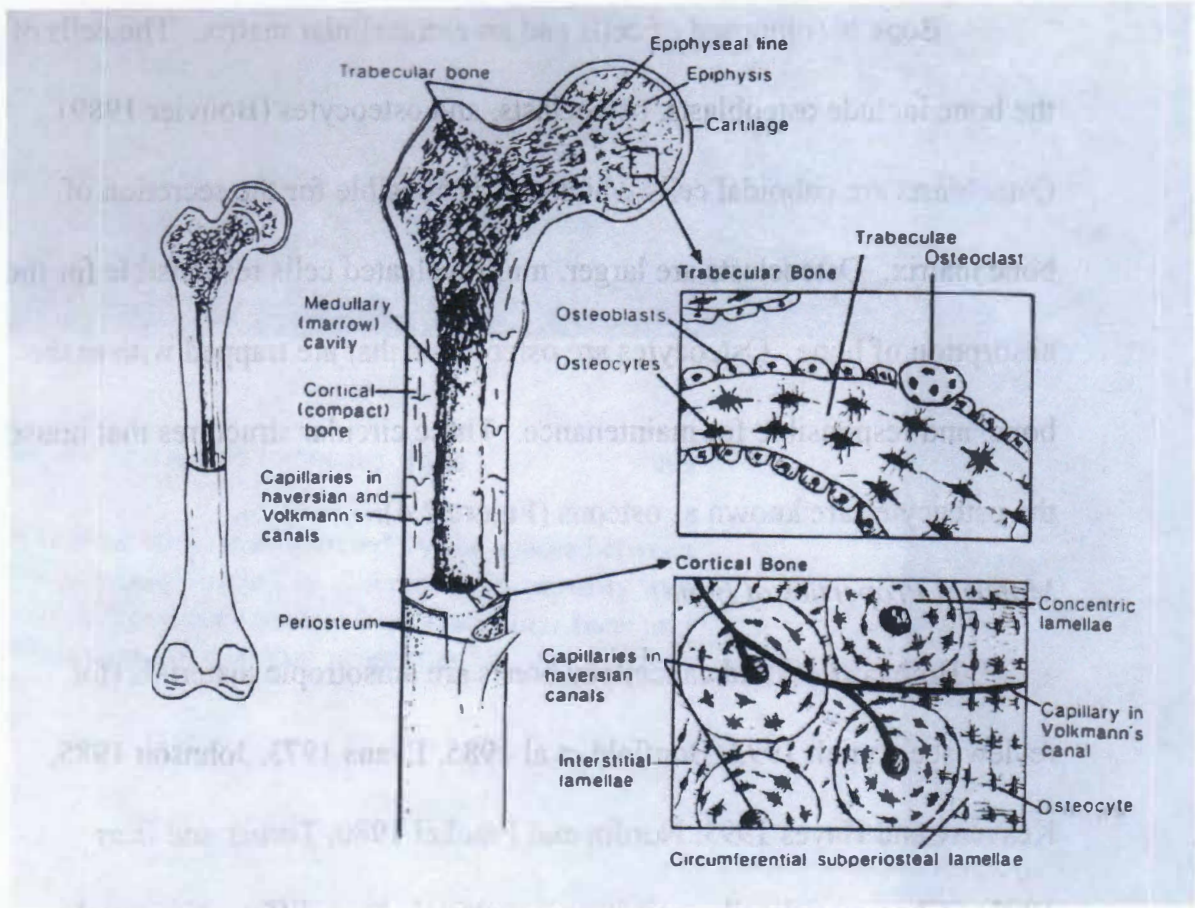

Figure 2.4. Structure and microstructure of human femur.

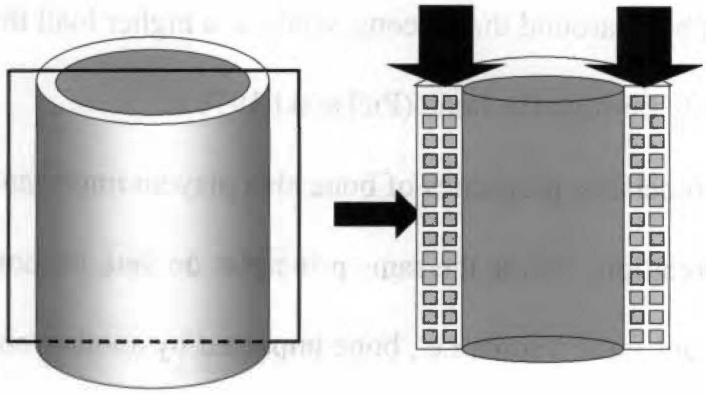

Figure 2.5 Anisotropic materials. Anisotropic materials have physical properties vary with direction; in this case, model is stronger in vertical than in transverse compression

(the direction the osteons run) than in the transverse direction. Human bone is also stronger in compression than in tension or shear. Human limbs and bone have adapted to constant compressive stressed from daily activity and have a higher resistance to compression than tension.

Human bone is also a viscoelastic material (for review see Bonfield and Li 1965, Keaveny and Hayes 1993, Piekarski 1970, Turner and Burr 1993). A viscoelastic material behaves in different ways depending on the rate and the length of loading. Cortical bone is extremely sensitive to strain. Cortical bone absorbs a large amount of energy from a normal activity such as running a mile. However, if less energy is applied all at

once, such as landing from a long fall, the failure level is reached and a fracture results. Histologically, fractures induced by low strain rate follow the interstitial bone around the osteons, while at a higher load they travel indiscriminately through the bone (Piekarski 1970).

The viscoelastic properties of bone also play an important role in trauma interpretation. While the same principles operate for both ballistic trauma and blunt force trauma i.e., bone impacted by another object, the resulting fracture patterns are quite different (Berryman and Symes 1998). The difference is due to the rate of loading. Blunt force trauma impacts bone at miles per hour while a ballistic projectile impacts bone at feet per second (Symes et al 1989). Keaveny and Hayes (1993) state that at high rates of loading, bone can behave like a brittle material skipping the stage of plastic deformation and failing quickly under the force.

Bone Deformation

Bone under stress and strain reacts in a predictable manner as outlined extensively by Keaveny and Hayes (1993), Nordin and Frankel (1980), Turner and Burr (1993). The deformation of the material has a direct relationship to the force of the load exerted upon it. This relationship is depicted as a stress-strain or load-deformation curve (Figure 2.6). Load-deformation curves depict the stages that bone undergoes through out

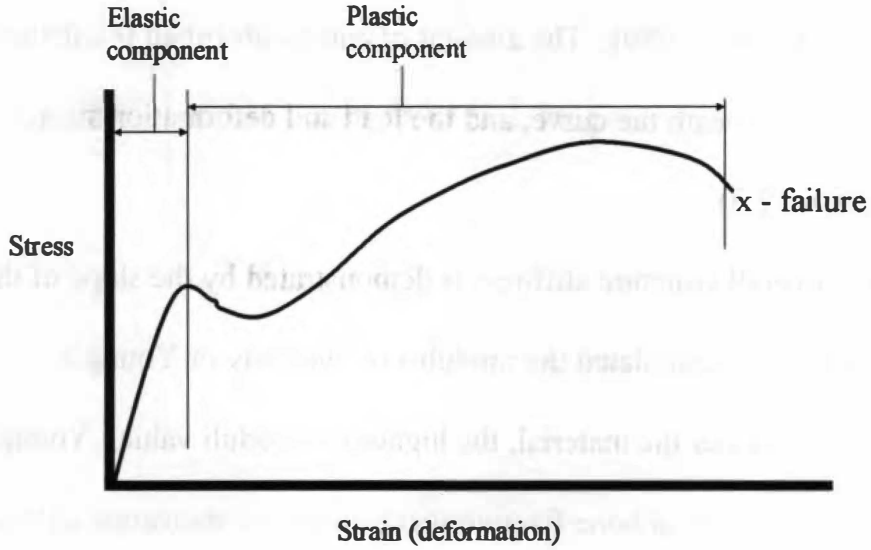

Figure 2.6 Diagram showing a typical stress-strain curve showing the elastic and plastic deformation phases and failure point (after Turner and Burr 1993: 597).

loading. The elastic deformation region is the first area of the load-deformation curve. When bone is in elastic deformation and the load is removed the bone will return to its former shape with no visual structural alteration. Bone enters the plastic deformation stage when a load has been reached. After release of the force, bone in the plastic deformation stage cannot return to its original shape even though fracture may not have occurred.

Load-deformation curves provide information on the amount of energy absorbed, load sustained, and deformation achieved before failure (Nordin and Frankel 1980). The amount of energy absorbed is calculated by the area underneath the curve, and the load and deformation sustained at failure (Figure 2.7).

The overall structure stiffness is demonstrated by the slope of the curve. Stiffness is calculated the modulus of elasticity or Young's modulus. The stiffer the material, the higher the moduli value. Young's modulus is important in bone fracture mechanics to demonstrate stiffness or

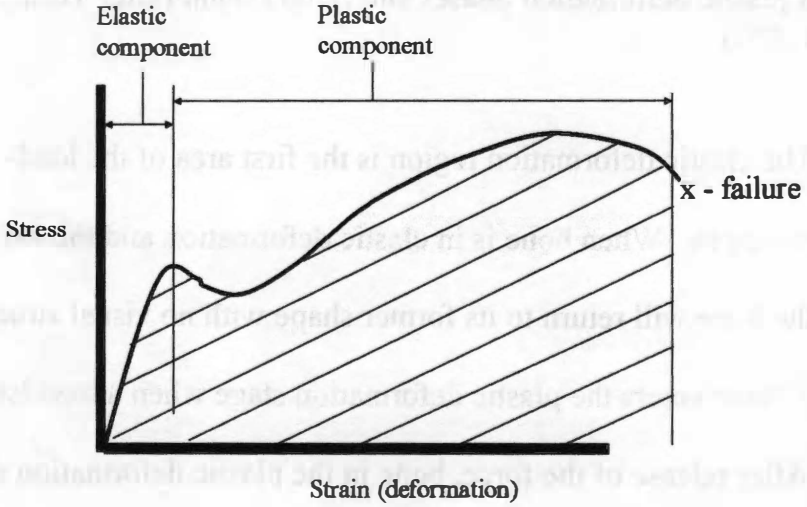

Figure 2.7 The absorbed energy before failure is calculated by the total area under the curve (After Turner and Burr 1993: 597).

ductility, which has a great influence on fracture mechanics. Brittle materials deform very little before failure, while ductile materials can withstand a great deal of elastic deformation. Brittle materials do not undergo plastic deformation when force is applied, and often require little force to reach failure.

Reaction to Tension

When equal loads are applied in a direction outward from the bone surface, tension is created. Maximum tensile stress occurs in a direction perpendicular from the applied force (Nordin and Frankel 1980). This force causes the material to narrow and lengthen. In bones, failure occurs at a microscopic level by the pulling apart of the osteons at the cement lines (Nordin and Frankel 1980).

Blunt Trauma and the Cranium

The analysis of cranial blunt trauma is slightly different than long bones. While the same biomechanical principles of biomechanics govern cranial fractures, there are differences in the structure and architecture of the cranium that deserves special consideration. The skull is composed of 22 separate skeletal elements that act as an entire system. The bones of the neurocranium vault are characterized as flat or irregular bones and are

formed in three layers, the inner and outer cortex (similar to cortical or lamellar bone) and the diploe, or spongy, cancellous bone in between.

The construction of these distinct layers affects the manner that fractures propagate through the skull. When a blow is delivered to the outer surface, the inner cortex is subjected to a greater degree of tension than the outer cortex. A micro-fracture often occurs on the inner surface directly below the impact site and then spreads to the outer surface and propagates from impact (Figure 2.8) (Mortiz 1954).

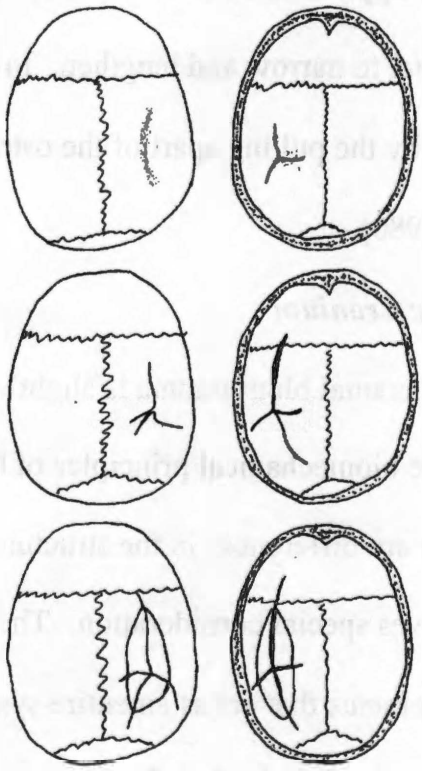

Figure 2.8 – Fracture propagation in both the inner (right) and outer (left) tables of the cranium. After Moritz 1954: 342.

The fractures traveling out from the point of impact in a linear direction are radiating fractures. As they move, secondary areas of tension and compression are created, and circumventing fractures i.e., concentric fractures transect the radiating fractures (Figure 2.9).

When the skull is entrapped between the impact and another surface, contrecoup fracture can occur. The coup/contrecoup phenomenon was first described by Hippocrates over 2000 years ago, and is described as a pattern of injury resulting from both the impacting blow, and the resulting impact against the opposing surface (Hein and Schulz 1990). Contrecoup injuries are seen in the brain, when a blow causes the brain to shift and impact the

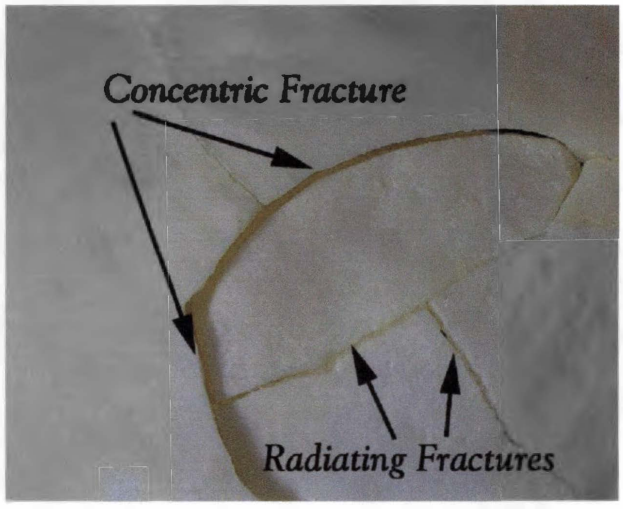

Figure 2.9. Concentric and Radiating fractures from blunt force trauma impact site to the left parietal (10X).

opposite side of the skull. Analysis of coup/contrecoup fractures requires that the anthropologist take into account both the blunt force trauma from the initial impact, and the blunt force trauma from the entrapping surface.

Chapter 3: The theories of E.S. Gurdjian and colleagues

One of the most enduring trauma studies in medicine was conducted in the 1940's and 1950's by ES Gurdjian et al. Gurdjian was a neurosurgeon and an anatomist interested in looking at the fracture patterns and mechanics of trauma in the human cranium. Gurdjian's conclusions were based on experimental and case review studies. Gurdjian and coworkers developed a variety of experimental designs and techniques which he used to address fracture propagation in the human skull.

Gurdjian and the Stresscoat technique

Gurdjian and colleagues began their research on blunt trauma in 1945 by looking at induced fracture lines in dogs, monkeys, and dry human skulls. During this study, Gurdjian developed his methods of using "stresscoat," a dry brittle lacquer, to stimulate bone. Stresscoat was designed to denote tensile strain in the material that it coats (Evans 1970). This was done to determine the areas of the skull that were under the most stress from blunt force impact. In the pilot study, dogs and monkeys were used to test stresscoat, and to determine if there were any differences in stresscoat fractures between living animals, recently dead animals, and completely dried skulls. Both monkeys and dogs were subjected to trauma while still alive and after death.

In order for stresscoat to function, the scalp and musculature were resected; the exposed skull buffed with sandpaper, the surface dried with ether, a layer of aluminum lacquer was applied, followed by a layer of stresscoat. Once the stresscoat was dry, the skull of each animal was impacted with an 8 ounce ball peen hammer. After impact, the animal was euthanized, and skull retained and examined. In order for the cracks in the stresscoat to be clearly visible (as the skull did not fracture) a dye etchant was applied to highlight the cracks, which were then traced with an India ink pen for photographic purposes (Figure 3.1) (Gurdjian et al 1945).

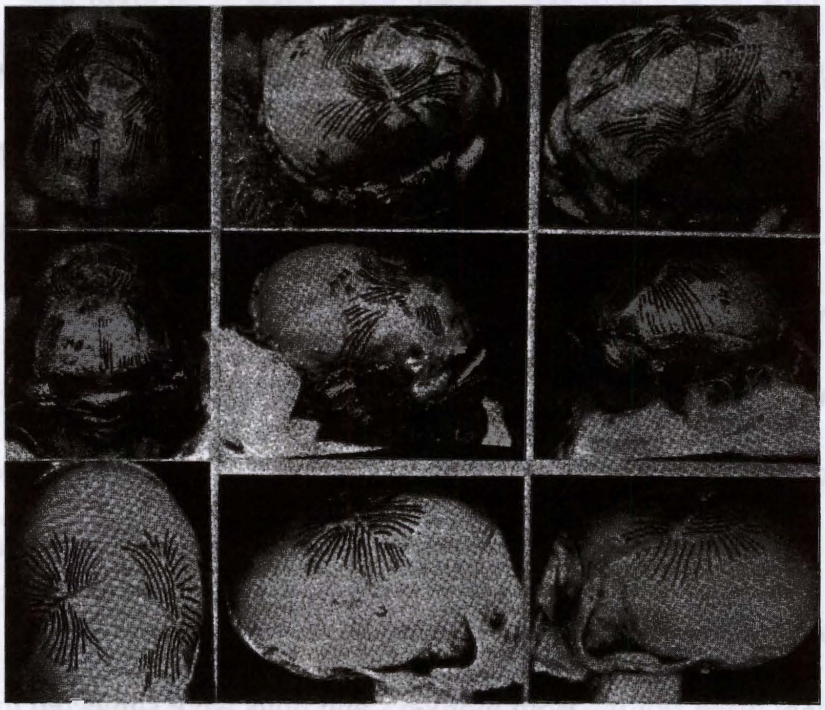

Figure 3.1 Views of Macaque skull after impact with the cracks in the stresscoat highlighted with India ink. From Gurdjian et al 1945: 681.

The same method was performed on each recently dead animal, with all cranial contents intact. The study was also replicated on the dry skulls (Gurdjian et al 1945). Gurdjian felt that a comparison of all three groups showed similar fracture patterns in the stresscoat, and from this he concluded that "a study of strain patterns based on dry skull preparations is accurate and represents conditions similar to those obtained in the living organism" (1945: 687). At this point in time, he felt that there were no biomechanical differences between dry bone, wet bone, and living bone. This conclusion opened a gateway for more studies that allowed the use of dried human skulls instead of fresh.

A secondary study was conducted on five dried human skulls and three embalmed cadaver skulls with all cranial contents intact. All skulls were impacted with a hammer while stationary on a steel slab. Gurdjian and coworkers (1945) noted that the sutures did cause concern amongst researchers, but proved to be of no influence to the data, as they seemed well sealed with stresscoat. Aside from sutures, Gurdjian also identified several other potential problems with the study. First only the external skull surface of the skull was evaluated and only regions of tensile strain were highlighted. Second, the dried skull surface was directly impacted with no soft tissue covering. In his next series of experiments, Gurdjian

tried to rectify those concerns and altered the experimental design. For his 1947 study, fresh cadaver skulls were used. The skulls were defleshed, "boiled for hours," and allowed to dry before experimentation. After cleaning with ether, the external and internal surfaces were coated with aluminum sealant and stresscoat. Once dry, each skull was suspended above a polished steel block by a silk thread. Instead of striking the skull with a hammer, the skull was dropped onto the block in the designated area and caught on the rebound to prevent further damage. The amount of force (*force = mass x acceleration*) exerted on the skull was calculated by using the weight of the skull and the drop height.

After impact, each specimen was sagittally sectioned using circular saw. Cuts were made in different planes dependent on the impact site. Again, cracks in the stresscoat were highlighted with a dye etchant and marked with ink. By looking at both surfaces, Gurdjian felt that he better understood the total stress on the skull. Any cracks on the internal surface (denoting tension) were taken to signal compression on the external surface. Bending was understood to produce tension on one surface and compression on the other. While Gurdjian (1947) felt this study improved greatly on the previous methodology, he noted that further studies isolating specific regions of the skull were required (1947).

In his 1949, 1950a, 1950b and 1953 studies Gurdjian held true to the stresscoat technique while adding a quantitative effort. In this research, the dry skull was coated with both internally and externally with stresscoat. The skull was sub-divided by region to better interpret fracture biomechanics and patterns. The twelve sub-regions included midfrontal, anterior interparietal, posterior interparietal, midoccipital, frontal lateral to the midline (left and right), anterior parietal (left and right), posterior parietal (left and right) and parietoccipital (left and right) (1950b). Each section was roughly 2 x 3 inches. Each region was impacted by dropping the skull onto a "heavy steel slab" which was placed directly on the lab floor. Again, the weight of the skull and the drop height was used to calculate the force of the impact. After impact the stresscoat was examined for cracks.

After analysis was conducted on the dried skulls, fully fleshed, embalmed cadaver heads were tested. They were also dropped onto a 160 pound steel slab placed directly on the floor (1950b). After testing, each head was processed and photographed for comparison with the stresscoat tests.

Gurdjian's Findings

From his serial stresscoat studies, Gurdjian and colleagues developed a suite of theories to explain the biomechanics of skull fractures. His theories include the patterns and direction of fracture propagation and the supporting mechanics. His first conclusion was that there is no biomechanical difference in fracture between dry, fresh, and living bone. He found a similar biomechanical fracture response for all three groups, with identical fracture patterns occurring. This finding enabled the extrapolation of trauma patterns from dried skull to living skulls.

From the stresscoat fractures (not in the skull), Gurdjian proposed that the skull develops areas of outbending and inbending as the result of blunt force impact. The blow causes an inbending of bone directly impacted and an area outbending of the surrounding bone. These areas of outbending experience high loads of tensile force, causing fracture. Fractures often initiate in areas that are remote to the point of impact, then radiate back towards it. This is because the "outbending is selective and may be localized to a certain part of the skull where a linear fracture is initiated due to the resultant tearing-apart forces" (1950b: 313). This area of outbending could "occur at a considerable distance from the point of application of the blow" (1950b: 313). Gurdjian even noted that the area of

greatest outbending may even be diagonally opposite the point of impact (1950b). This pattern was described as "an undulating type of movement with simultaneous inbending in the region of impact and outbending at the border of the area of inbending" (Figure 3.2) (1947)

Initial failure was proposed to start in this region of outbending. Once fracturing begins, it extends towards the point of impact and in the opposite direction (1950b). In other words, the direct impact of the skull caused deformation in the other areas resulting in failure first in these areas

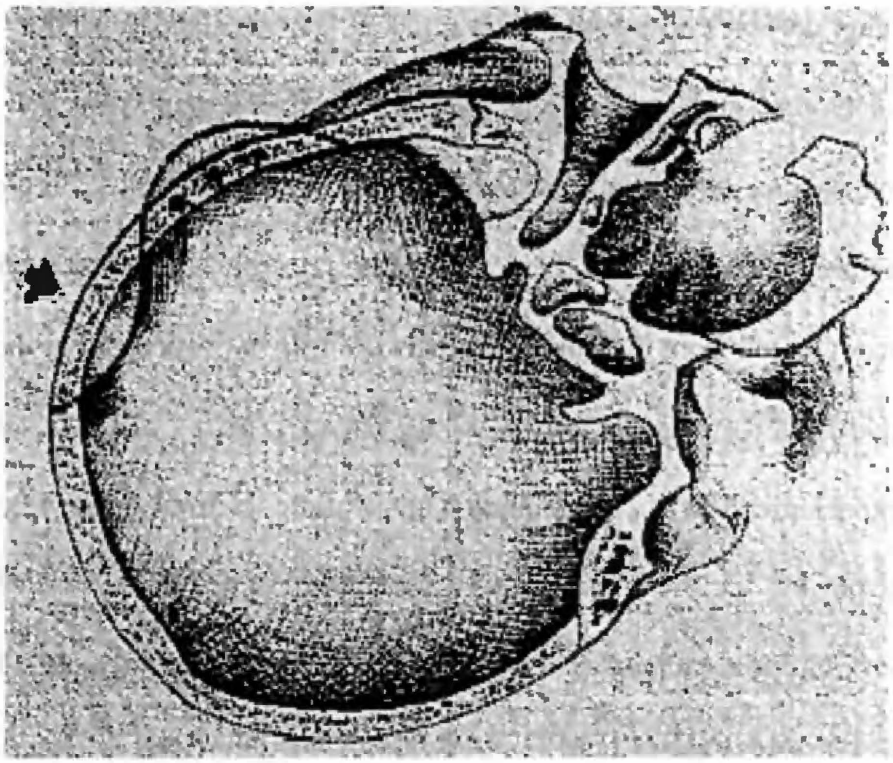

Figure 3.2 The areas of inbending and outbending associated with impact site. From Gurdjian 1949: 738

and then the fracture traveling back towards the impact site. Gurdjian reiterated that "the cracks appear on the outside of the skull in the regions in which the bone bends outwards" and initial fractures "may occur at a considerable distance from the point of the application of the blow" (1950b: 313). The forces caused a fracture to begin quite a distance away from the point of impact. Multiple fractures could occur in different locals and each radiate back towards the impact site (1947).

Gurdjian also evaluated the differential behavior between the inner and outer cortexes of the skull after impact. He noted and extensive presence of what he described as a stellate or star like pattern on the internal surface of the skull in the direct area of impact (1947). In contrast to fractures initiating at the areas of outbending, the cracks on the internal surface radiated from the point of impact. Gurdjian proposed that this resulted from the strain of impact, which he suggested, traveled away from the impact site (1947). The stellate pattern often occurred on the internal surface of the skull with out any corresponding failure of the outer cortex. In short, Gurdjian demonstrated that the internal surface of the skull failed before the outer surface (1947). Failure was first shown by the crack in the stresscoat on the inner cortex then as those ended the cracks in the outer

cortex began. He also noted that it was possible to get a tearing of the bone layers caused by shear forces (1947).

The experimental studies also revealed that fracture patterning and propagation was influenced by the curvature and the buttressing of the skull. The radiating fractures were noted to follow the area of the skull with the least amount of curvature. Fractures also avoided heavy buttressing or reinforcement in the skull. This created a fracture pattern following a linear nature along the flatter regions of the cranial vault.

Using these principles of fracture propagation, Gurdjian outlined fracture mechanics for impacts in each of the eight regions described. All patterns were described after testing with stresscoat and based entirely on this method (Gurdjian 1950b).

Midfrontal – Impact to the midfrontal region produced failure in the midline frontonasal suture, above the orbits, and superorbital notches. The fractures then traveled posterior (or dorsal) towards the impact site. Fractures to the maxilla in the vicinity of the infraorbital notch were also noted (1953).

Anterior Interparietal Area - Blows to this region produced primary failure areas in either parietotemporal regions.

Posterior Interparietal Area – Impacts initiated failure first in a circular pattern around the impact site and secondary failure lateral to it.

Midoccipital Area – Failure was noted to begin from "side to side" in the base of the skull. Fracture patterns consistently begin at the foramen magnum and travel towards the point of impact. If more energy was applied, additional fractures radiated from the parietal region back toward the impact site.

Frontal Area Lateral to the Midline – The stresscoat indicated that fractures began in the orbital roof and the root of the zygomatic arch.

Anterior Parietal Area – Stresscoat fractures began in the temporal region, defined as the "weakest" region and extend superior toward the impact site.

Posterior Parietal Area – Fractures initiated in the temporal frontal region and extend back towards the point of impact.

Lateral Parieto-Occipital Area – Blows to this region formed fractures in the cranial base that radiated superior toward the impact site. Stresscoat fractures were also seen "extending from the region lateral to the foramen magnum to the point of impact" (1950b: 323).

Gurdjian's Followers

Gurdjian published extensively on this pioneering technique and results. His theories were universally applied to trauma interpretation. His

articles encouraged the scientific community to use the findings as a predictive template for impact site. He noted, "on the basis of this study it should be possible to predict the position of the fracture line fairly accurately when the location of the blow is knows; or if the fracture line is found on the x-ray film, the position of the blow producing it may be determined" (1949: 741). With this promise, forensic pathology and anthropology has held fast to Gurdjian's work and standards.

Berryman, Symes, and Smith (1991) have produced a large body of trauma research in the field of forensic anthropology. Their analysis of forensic specimens provides a wealth of biomechanical exemplars. The use of Gurdjian's models can be seen in their explanation for blunt force fracture patterns. Berryman and Symes (1998) demonstrate that fracture patterns are often created with the initial fracture formation occurring in the area of outbending, remote from the point of impact. In "Broken Bones: Anthropological Analysis of Blunt Force Trauma," Galloway (1999) also agrees with Gurdjian's findings, stating that fracture initiation may begin at a site distant from impact, due to considerable outbending of the bone (1999).

Forensic pathology has also been dependent upon Gurdjian. DiMaio and DiMaio (2001), a standard in the field, used Gurdjian as the basis for

blunt trauma interpretation. They state that the area of impact is bent "inward" while "adjacent and more distant areas are bent outward" (2001: 149). The area of outbending was where the first fracture could occur and as DiMaio notes this "occurs at quite some distance from the area of inbending" (Figure 3.3) (2001: 148).

Knight (1996) also refers to Gurdjian in his explination of blunt force trauma fracture patterning in the skull. He notes that after a blunt impact, there is "suprising large" deformation to the shape of the skull (1996: 180). Knight refers this deformation as the "struck hoop" analogy (Figure 3.4).

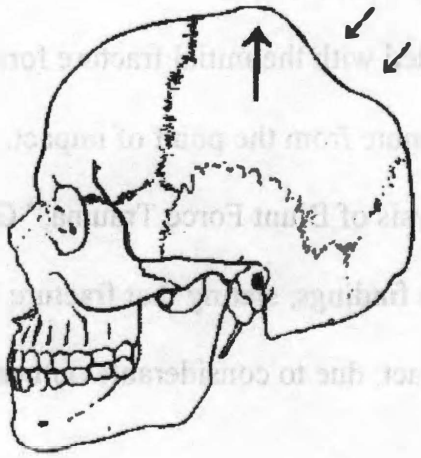

Figure 3.3 Left lateral view of the skull demonstrating the inbending and outbending that occurs from blunt impact. (after DiMaio and DiMaio 2001: 148).

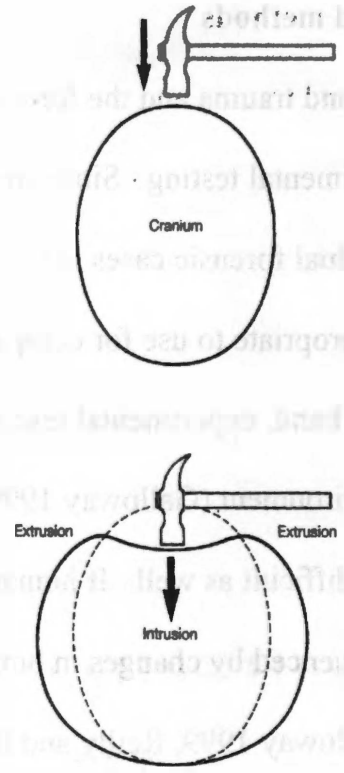

Figure 3.4 – An illustration of the "struck hoop" analogy that Knight adapated from Gurdjian. (Knight 1996: 180).

Examples and illustrations such as these show the heavy reliance of the forensic community on Gurdjian. His theories and research have had and enduring effect on forensic science and fracture pattern interpretation.

Chapter 4: Material and methods

In order to understand trauma and the forces used to inflict it, anthropologists use experimental testing. Since the exact mechanism or force of trauma for individual forensic cases may never be known, they are difficult and may be inappropriate to use for comparative purposes and publication. On the other hand, experimental testing can provide a wealth of data in a controlled environment (Galloway 1999). However, experimental designs are difficult as well. If human cadavers material are used, the data may be influenced by changes in bone quality caused by embalming or drying (Galloway 1999, Reilly and Burnstein 1974). Bone quality can also be compromised by age as density decreases (Bonfield 1985, Oxnard 1993). Soft tissue presence and/or condition influences the biomechanics, especially in the cranium (McElhany 1976). Removal of soft tissue from over the impact site alters the elastic and biomechanical properties. Experimental testing is also restricted by the availability of cadaveric material. Sample sizes may be small and limited in age, race, and sex representation.

Despite these problems, experimental testing can answer questions about fracture patterning and bone trauma (Galloway 1999, Yoganandan et al 1995). Specific problems can be addressed and supporting data

collected. Because environment is controlled, variables can be carefully manipulated and the results of trauma studied.

Research in industrial/biomedical engineering routinely uses impact testing to understand material deformation under set loading conditions. The energy and force absorbed by the specimen are calculated and recorded. An impact-testing model was chosen for this study because it replicates blunt trauma and provides information on the biomechanical response of the bone to the load. Impact testing affords the highly unique opportunity to monitor the cranium's response during impact. Recent advancements in instrumented impact testing allow quantification of the axial load, shear force, and the moment of the impact for every millisecond of the event.

Instrumented impact testing, as employed in this model, is commonly used to determine load vs. deformation of a material such as bone under high speed impact. The standard protocol for this test involves construction of a steel "drop tower" structure that allows for controlled and monitored descent of weight with an attached instrumented load cell (Figure 4.1). The computer monitors load and collects of information like deflection, elastic stiffness, maximum load, absorbed energy, damage, and load at failure (Turner and Burr 1993). The impactor cell record the data of

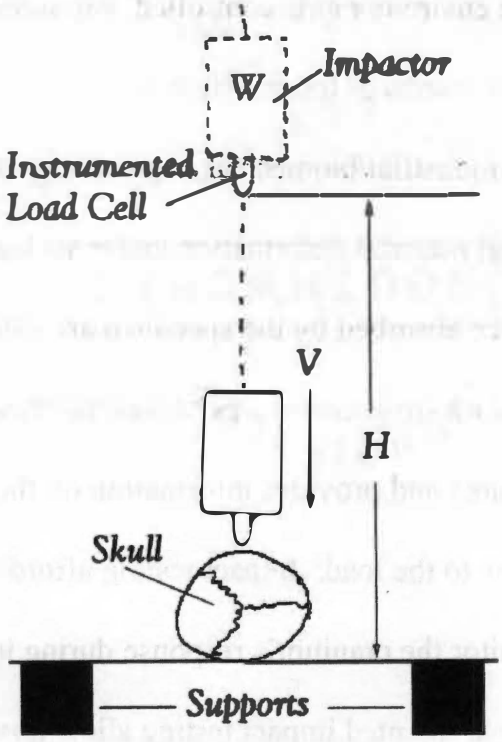

Figure 4.1. Set up of a standard drop tower structure. The weight (*W*) of the impactor and the height (*H*) of the fall are used to calculate the resulting velocity (*V*).

the force throughout descent and impact, which is recorded as the impact load *P*, a continuous function of *t* time (Turner and Burr 1993).

In the experimental test setup, several load cells recorded the data. Two support load cells were used with a thin, scored board across them. The board was used to orient the skull with the parietal directly below the impactor. The board did not affect the data and broke away immediately on impact, allowing the head to have free movement away from the impactor.

Data was recorded from the four separate load cells (Figure 4.2). Both supports had inline load cells to measure axial response from the impact event. The impactor measured axial load as well as shear loads and moments from the Y and Z axes. For the impactor load, however, only the axial load was used as moment and shear force data was considerably smaller than the resulting axial load. The data from the impactor load cell was inertially compensated, to correct for the standard inertia of the fall. Compensation was necessary due to the fact that as the impactor hits the skull it is accelerated upwards (decelerated) as the event proceeds.

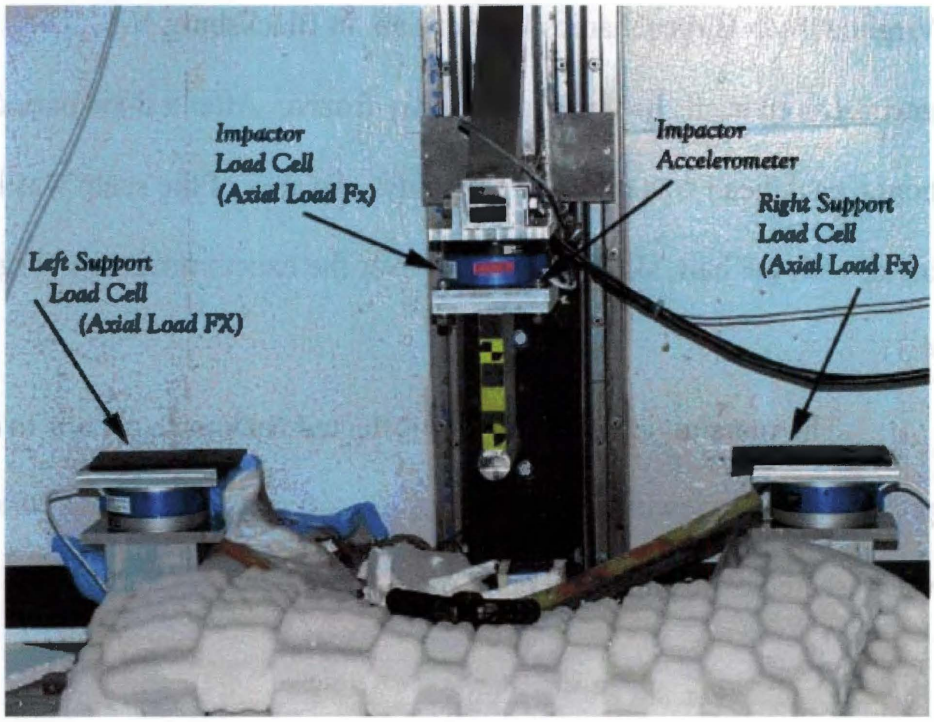

Figure 4.2 The location of load cells.

Data from the load cells was recorded from –30milliseconds (ms) to 300ms, with 0ms being the time at which the impactor triggered the data acquisition system via a trigger strip mounted on the head. The time of bony impact is not exactly at 0ms since the trigger strip was placed on top of the soft tissue and hair. Data from all load cells was captured pre- and post- trigger to ensure the entire event was recorded. Data were acquired through a series of channels, and imported into an Excel spreadsheet.

Specimens

To test fracture propagation in the neurocranium, five cadaver heads, 2 females and 3 males ranging in age from 61-89, were obtained from Virginia Tech Biomechanics Impact Lab, in Blacksburg VA. The unembalmed heads had been previously frozen. After a thaw period of 36 hours, each head was prepared for study. An area of the scalp was left intact with the hair, skin, and muscle over the exact impact site (Figure 4.3).

The remaining soft tissue was reflected back in four flaps to enable proper fracture viewing and imaging. All soft tissue, including periosteum, was resected exposing clean bone.

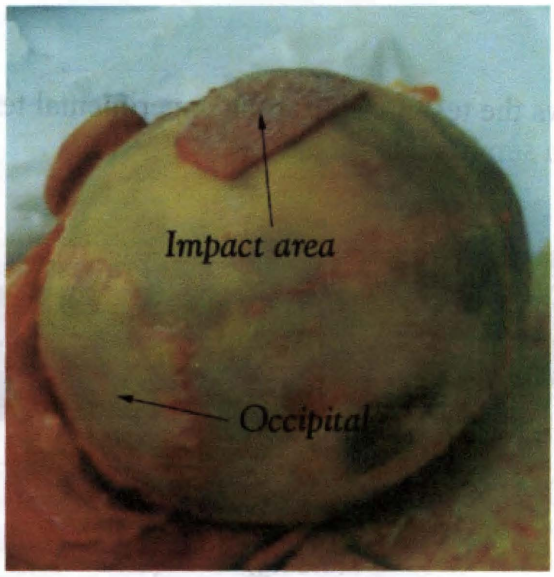

Figure 4.3 Impact area on left parietal with intact soft tissue, and clean bone on the rest of the cranium in a head ready for testing.

Head weights ranged between 8.84 lbs (3.3kg) to 14.20 lbs (5.3 kg) with an average of 4.26 lbs (Table 4.1). All skulls were impacted in the parietal region, corresponding to Gurdjian's Anterior Parietal region. Four were impacted on the left side and one on the right. The skull tested on the right side had a small degree of soft tissue damage to the left side, that may affected results. The parietal was chosen as the impact site for several reasons. First, in order to properly video capture the fracture progress, a site was selected that enabled viewing. Second, the parietal is of fairly uniform thickness. Third, there are no thick muscle attachment sites as in the occipital, and it is not nearly as thin and liable to punch through as the temporal. For these reasons, the high parietal was chosen to help insure

Table 4.1 shows the test matrix for the experimental tests. An * indicates test involving a semi-rigid boundary

Test	Gender		AGE	Pre-test Measurements			
	MALE	FEMALE		Mass of Head	Drop Height	Drop Mass	Overlap length
	3	2					
1		1	89	9.65 lbs (3.6 kg)	77 in (1.96 m)	23 lbs (8.58 kg)	2 in (5.08 cm)
2		1	61	8.84 lbs (3.3 kg)	111 in (2.82 m)	23 lbs (8.58 kg)	2.5 in (6.35 cm)
3	1		61	14.20 lbs (5.3 kg)	111 in (2.82 m)	23 lbs (8.58 kg)	3.5 in (8.89 cm)
4	1		71	11.79 lbs (4.4 kg)	111 in (2.82 m)	23 lbs (8.58 kg)	3.5 in (8.89 cm)
*5	1		61	12.59 lbs (4.7 kg)	111 in (2.82 m)	23 lbs (8.58 kg)	3.5 in (8.89 cm)

good fracture propagation instead of a simple depression fracture. Major suture structures were also avoided as they tend to absorb energy and alter fracture propagation.

The heads were placed in the drop tower structure and struck from a range of 77 in (1.96 m) to 111 in (2.82 m). An "overlap" was created to allow the impactor to fall further than the initial point of contact with the skull. Styrofoam squares were placed in the drop tower to slow down the impactor after the drop. The overlap height ranged from 2 in (5.08 cm) to 3.5 in (8.89 cm) (Figure 4.4). The drop mass was consistently 23 lbs

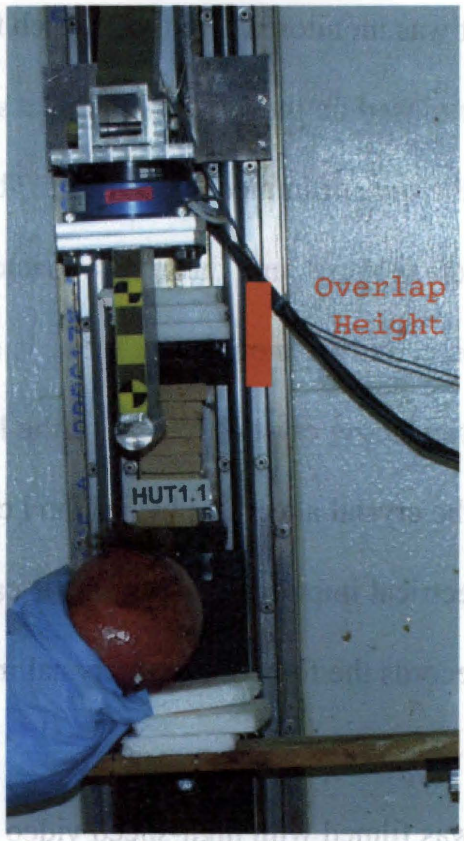

Figure 4.4. The skull positioning in the drop tower, with overlap height (distance impact is allowed to travel past contact with skull).

(8.58kg). The skulls were stabilized at the lower end of the drop tower by a 2x4 wooden board that was scored with a circular saw within 1 cm of the opposite side. Essentially, the board kept the skull off of the ground allowing it to break away upon impact and properly stimulating a blow to an unconstrained head. One test used a semi-rigid boundary to see if a different amount of energy was needed to produce a fracture in that situation.

The impact was monitored throughout each test by load cells. A trigger switch was placed on the top of the impact site to trigger sensor monitoring from the time of immediate contact. The force was measured off the right and left supports, and the axial impactor arm, which calculated axial and shear force, and the moment for the x, y, and z axis. These were measured by physioelectric crystals in each of the load cell sensors. Any force exerted on the crystal alters its physical and chemical properties sending out an electrical impulse. This charge is calibrated and received by a computer that records the force for each crystal in intervals of milliseconds.

Each test was filmed with high-speed video to show the exact fracture propagation. The video was placed to capture fracture propagation through the posterior parietal and occipital region. The high speed video was set to film faster than the fracture travels through bone (approximately 7,000 frames per second), allowing approximately 1.25 centimeters (cm) of fracture propagation per frame. This speed enabled viewing of fracture travel while still providing good resolution and definition. The video input was recorded digitally and input into the data acquisition computer.

After impact, each skull was cleaned, photographed, and diagramed. Due to time constraints, the skulls were not able to be processed and

reconstructed. However, as much soft tissue as possible was removed. The skull was examined for fractures in all areas, including locations remote to impact. All fractures were described, measured, and charted.

Chapter 5: Results

Many changes in the field of impact biomechanics have occurred since Gurdjian began his studies in the 1940's and 50's. New methods have emerged and technology has advanced greatly, allowing precise measurements of biomechanical response of bone to impact. Digital imaging technology is now at a state where fracture propagation can be captured, viewed, and studied (Hodgson et al 1970, Ketlinshi 1970). The stresscoat studies preformed by Gurdjian were innovative and advanced for that time. However, scientists should constantly re-test the standard theories with the latest technology to keep the knowledge current. Under that principle, the theories of Gurdjian were retested according to the impact biomechanics of today.

From each test run, fracture patterning was analyzed as well as the biomechanical response of the bone. In addition, the force over time P(t) as recorded by the load cell during the impact was analyzed.

Test One

Test specimen 1 is a female age 89, with head weight of 3.6 killograms (kg). The left parietal was impacted from a drop height of 77 in (1.96 m) and a weight of 23 lbs (8.58 kg). The impact caused two radiating fractures. The main radiating fracture traveled from the point of impact to

terminate into the squamosal suture, a total distance of 2.5 inches (6.35 cm). A secondary fracture radiated laterally a distance of 1.25 inches (3.175 cm) (Figure 5.1). All fractures recorded were radiating from the impact site. No fractures were noted to radiate back towards the impact site.

Data from load cells was analyzed. The axial load reached a force of 817 lbs (Figure 5.2). The first peak of the curve represents the initial bone

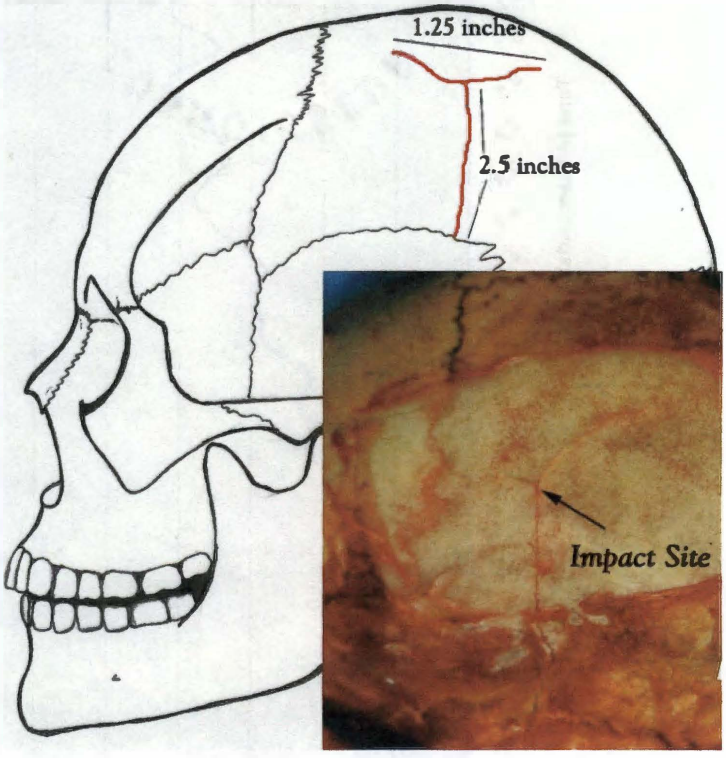

Figure 5.1. Fracture pattern in test one in the left parietal, with impact site 2 in (5.08 cm) from sagittal suture .6 in (1.52 cm) from coronal suture, and 2.5 in (6.35 cm) from the sqaumosal suture.

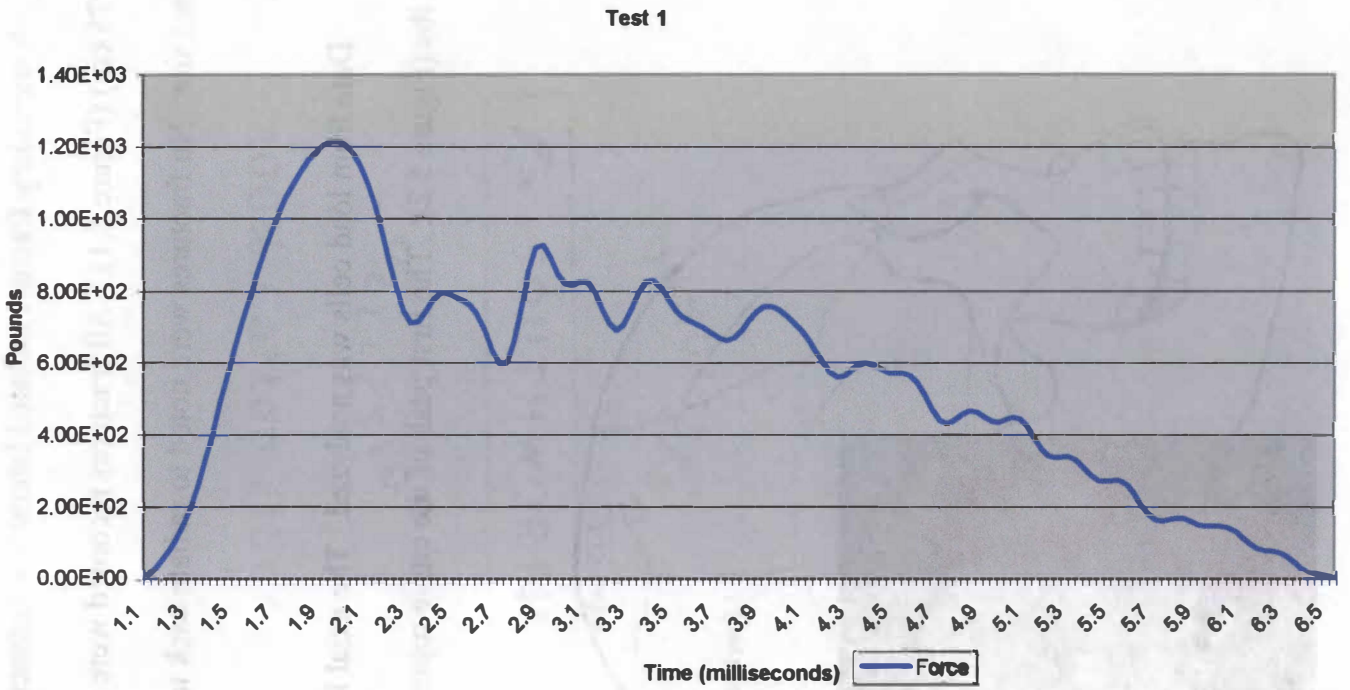

Figure 5.2 Force in pounds (recorded in scientific notation) to time in milliseconds for Test 1.

failure and the creation of the radiating fracture. This event occurred .966 seconds after impact. There are two secondary peaks present in the data that represent further release of energy. These may represent the creation of secondary radiating fractures. Both occur around at a force level of around 650 lbs. The sharp decline in the energy shows that the skull has been fractured. A comparison of the high speed video of the event demonstrates that at energy decline the skull was freely moving away from the impactor.

Test Two

Test specimen 2 is a 61 year old female with a head weight of 8.84 lbs (3.3 kg). The left parietal was impacted from a drop height of 111 in (2.82 m) with a drop mass of 23 lbs (8.58 kg). Fractures were formed at the point of impact and radiated into the sqaumosal suture traveling a total distance of 3.5 inches (Figure 5.3). Additional small fractures in the outer cortex were noted in a circular concentric pattern around the point of impact. No additional fractures radiating from locations other than the impact site were noted.

In addition to the visible fracture patterning, data from the load cell was also analyzed. The maximum axial load during the event was reported at 1140 lbs during the primary peak of the fracture event.

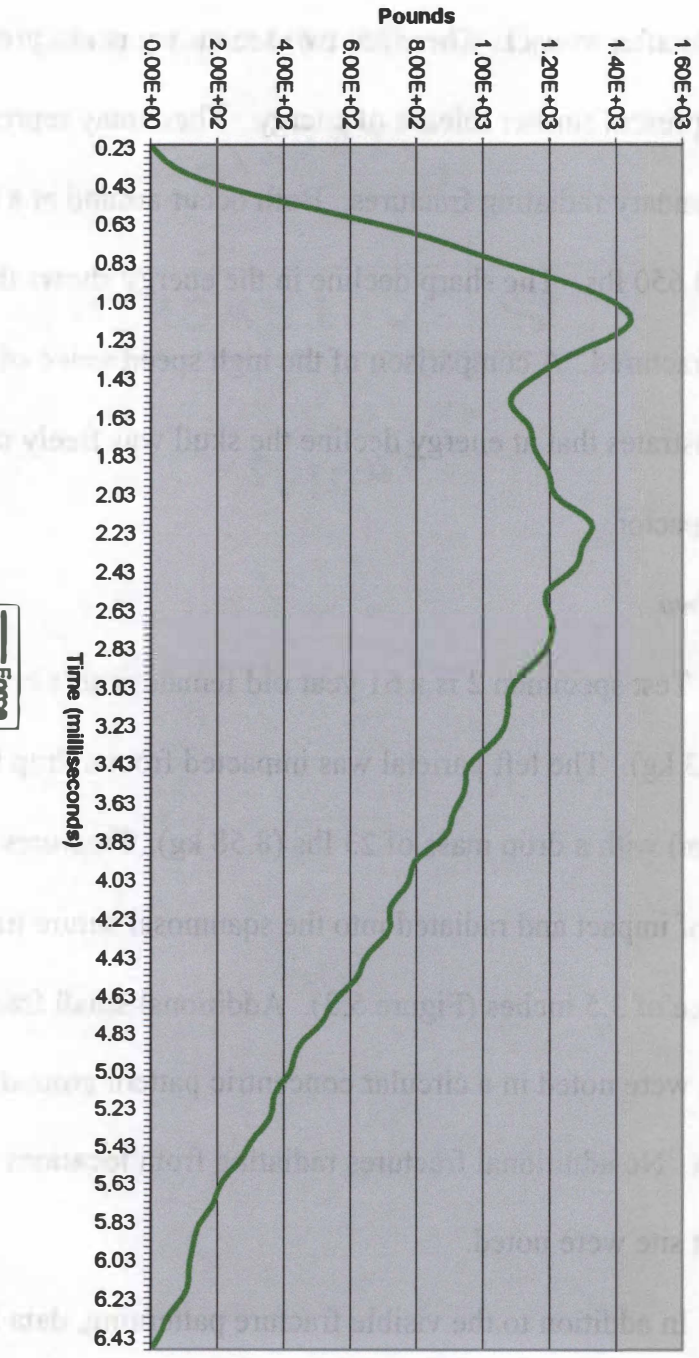

Figure 5.4 Force in pounds (recorded in scientific notation) to time in milliseconds for Test 2.

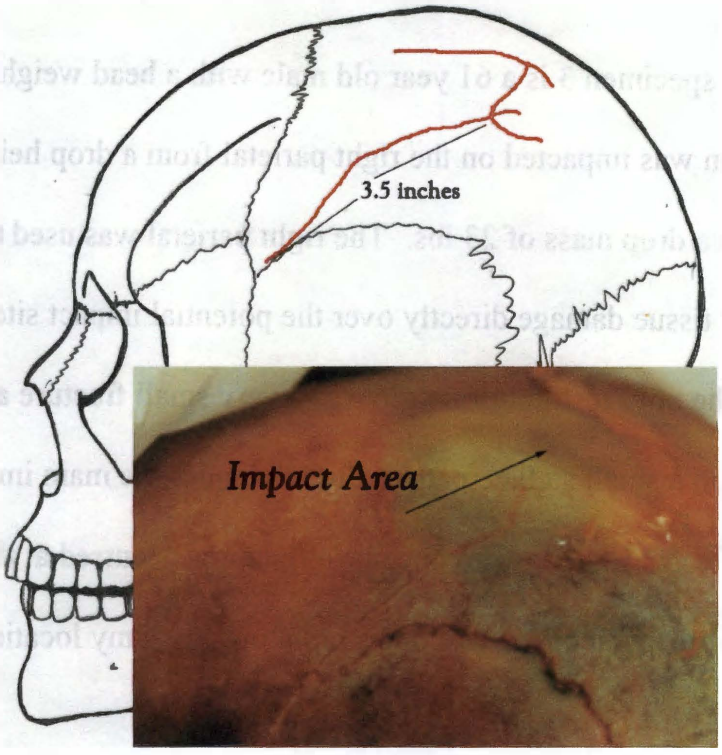

Figure 5.3 Fracture pattern in the left parietal for test two with an impact site 2 in (5.08 cm) from the sagittal suture, .75 in (1.91 cm) from the coronal suture, and 2 in (5.08 cm) from the sqaumosal suture.

This major peak represents the main failure point for the bone and fracture initiation (Figure 5.4). The earlier secondary peak may represent a microfracture, or failure of the outer or inner cortex. The major failure occurred at 1.1 seconds into the event. From a comparison of the fracture patterns and timed sequence of the data it is probable that the main radiating fracture was created at the force peak of 1140 lbs, with secondary fractures occurring at 800 lbs of force.

Test Three

Test specimen 3 is a 61 year old male with a head weight of 5.3 kg. The cranium was impacted on the right parietal from a drop height of 111 inches with a drop mass of 23 lbs. The right parietal was used to avoid an area of soft tissue damage directly over the potential impact site on the left parietal. The only resulting fracture was a very small fracture affecting the outer table in a small stellate pattern directly under the main impact site (Figure 5.5). No radiating or concentric fractures occurred at the impact site and no other fractures were notes radiating from any locations remote to impact.

While all impact variables were constant between test two and test three, vault thickness might explain the differential fracturing. Furthermore, specimen three is a large male with a skull weight of 14.20 lbs (5.3 kg).

The main fracture occurred after an applied force of 1400 lbs (Figure 5.6). This occurred 3.01 seconds into the event. There is an earlier peak in the data which could signal a microfracture or failure of the outer or inner cortex. This peak occurs around 875 lbs of force. After the main failure there was a swift loss of energy and analysis of the high speed video show that the skull was moving away from the impactor at this time.

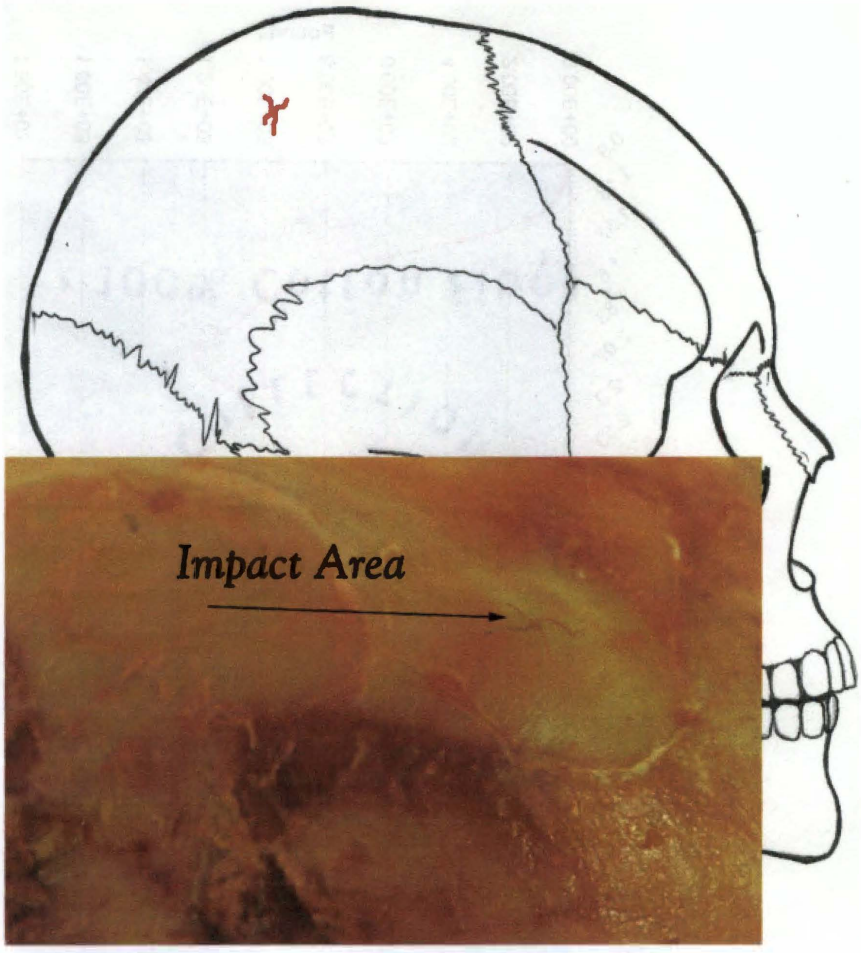

Figure 5.5 Fracture pattern in test three in the right parietal, with impact site 2 in (5.08 cm) from sagittal suture .75 in (1.91 cm) from coronal suture, and 3.5 in (8.89 cm) from the sqaumosal suture.

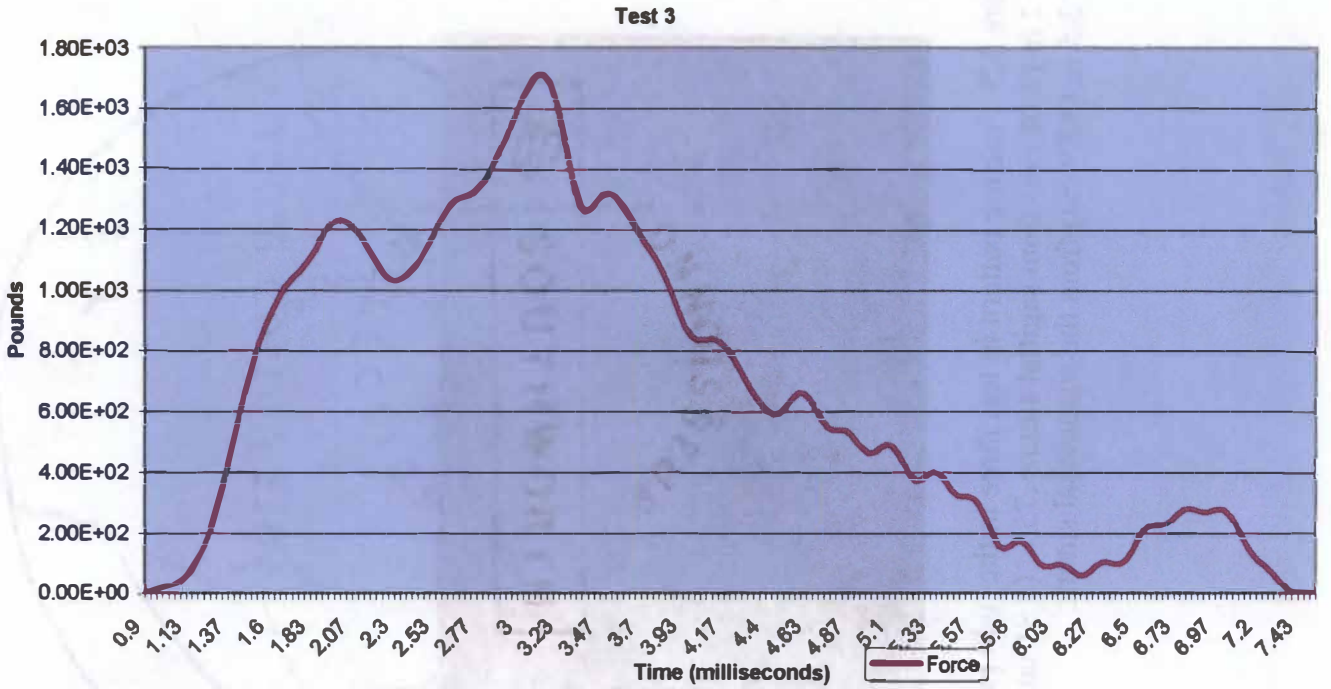

Figure 5.6 Force in pounds (recorded in scientific notation) to time in milliseconds for Test 3.

Test Four

Test four involved a 71 year old male with a total head weight of 4.4 kg. The drop height was 111 inches with a drop mass of 23 lbs. The left parietal was impacted with no visible fractures.

The data shows a peak at 1400 lbs of force (Figure 5.7). However no fracture resulted. There is a smaller peak at around 600 lbs of force, and it is possible that damage did occur but was contained within the inner cortex or hidden by soft tissue. The drop in energy is sharp and the high speed video shows that the skull moved from the impactor almost immediately.

Test Five

Test five tested the difference in fracture patterns between un-constrained impacted crania and those with semi rigid boundary. This test was conducted to see if the constraint of the skull would produce the fracture patterns similar to Gurdjian's findings. The board that stabilized the other four test subjects until impact was not scored in this test. The board doesn't completely constrain the skull but provided enough resistance to measure the differences. The semi rigid boundary was the only variable altered in the test. The drop height and drop mass remained constant.

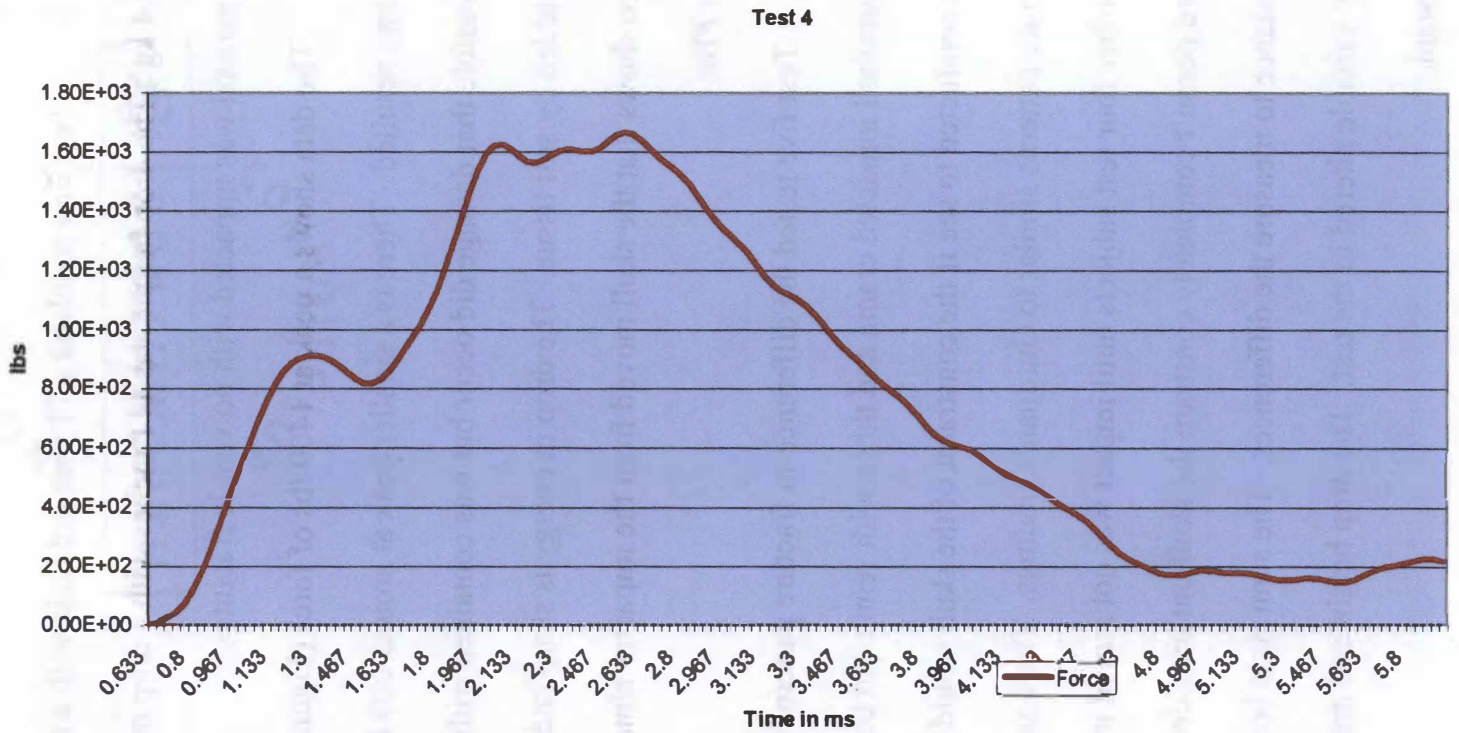

Figure 5.7 Force in pounds (recorded in scientific notation) to time in milliseconds for Test 4.

At impact, the board failed allowing the skull to move in the direction of the impact. However, the presence of the semi rigid boundary drastically changed the results of the test. The fracture pattern was different with two main areas of fractures occurring on the left parietal (site of impact) and the right parietal. Fractures are more complex with many radiating and concentric fractures present (Figure 5.8, 5.9). Bilateral fractures were also present through the frontozygomatic sutures (figure 5.10). The complex fracture patterns failed to occur at remote locations and travel back towards the impact site. Damage to the left side of the cranium results from direct impact and damage to the right results from the semi rigid boundary provided by the board. There was a noticeable difference between the data collected by the load cell data between the unconstrained and constrained tests. The event for the constrained test lasted considerable longer with several fracture events visible in the graph (Figure 5.11). The main peak occurs at 840 lbs of force but there are other major failures. Analysis of the high speed video show that the first peak indicates the failure in the area of the impact site with radiating fractures creating the release in pressure as indicated by the sharp drop after peak one. The semi rigid boundary created additional peaks in energy, indicating failure of the right parietal (side opposite from impact), and failure of the facial skeleton.

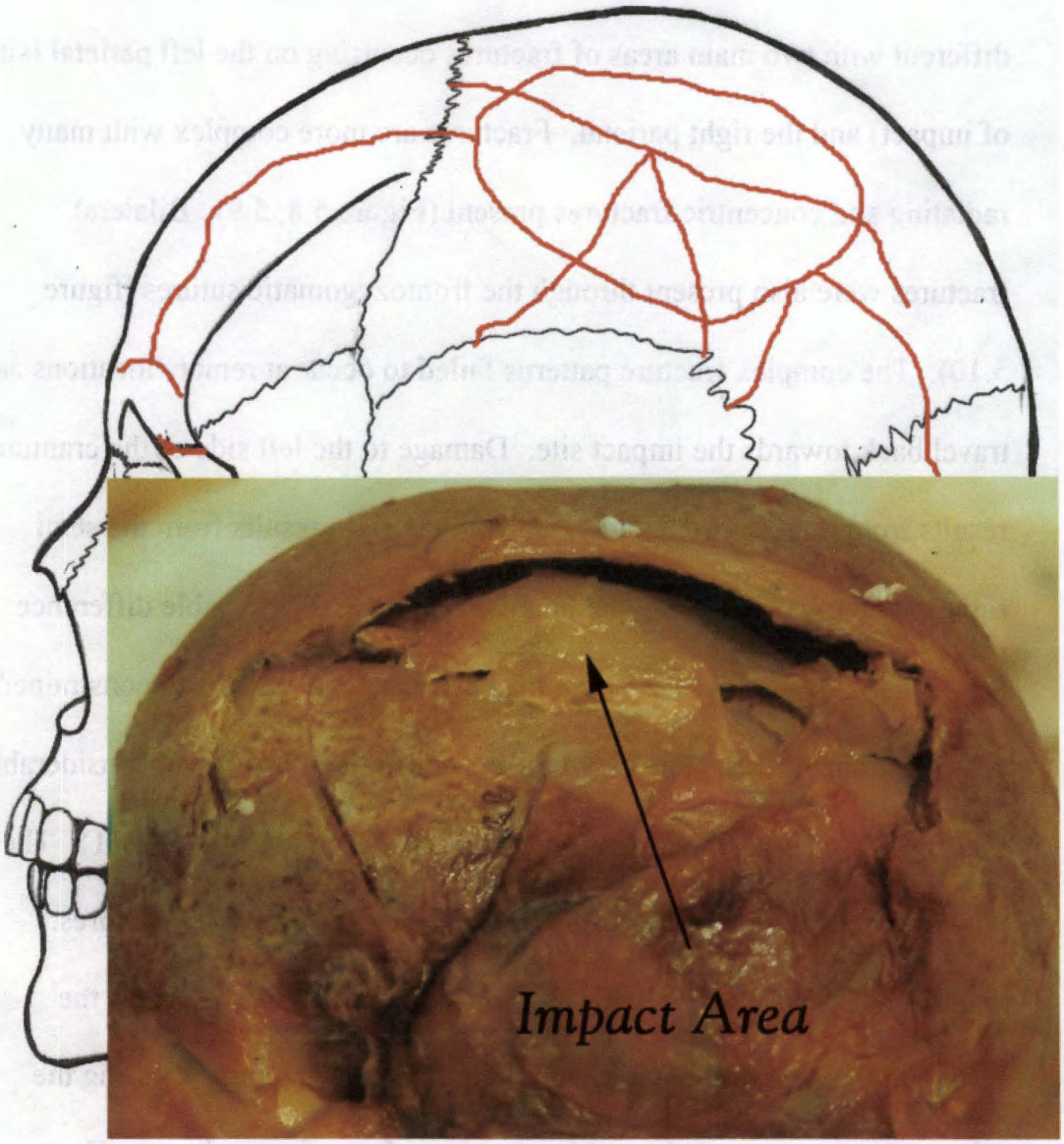

Figure 5.8 Fracture pattern in test three in the right parietal, with impact site 2.5 in (6.35 cm) from sagittal suture .75 in (1.91 cm) from coronal suture, and 3.5 in (8.89 cm) from the sqaumosal suture. Extensive fracture are present at the area of impact.

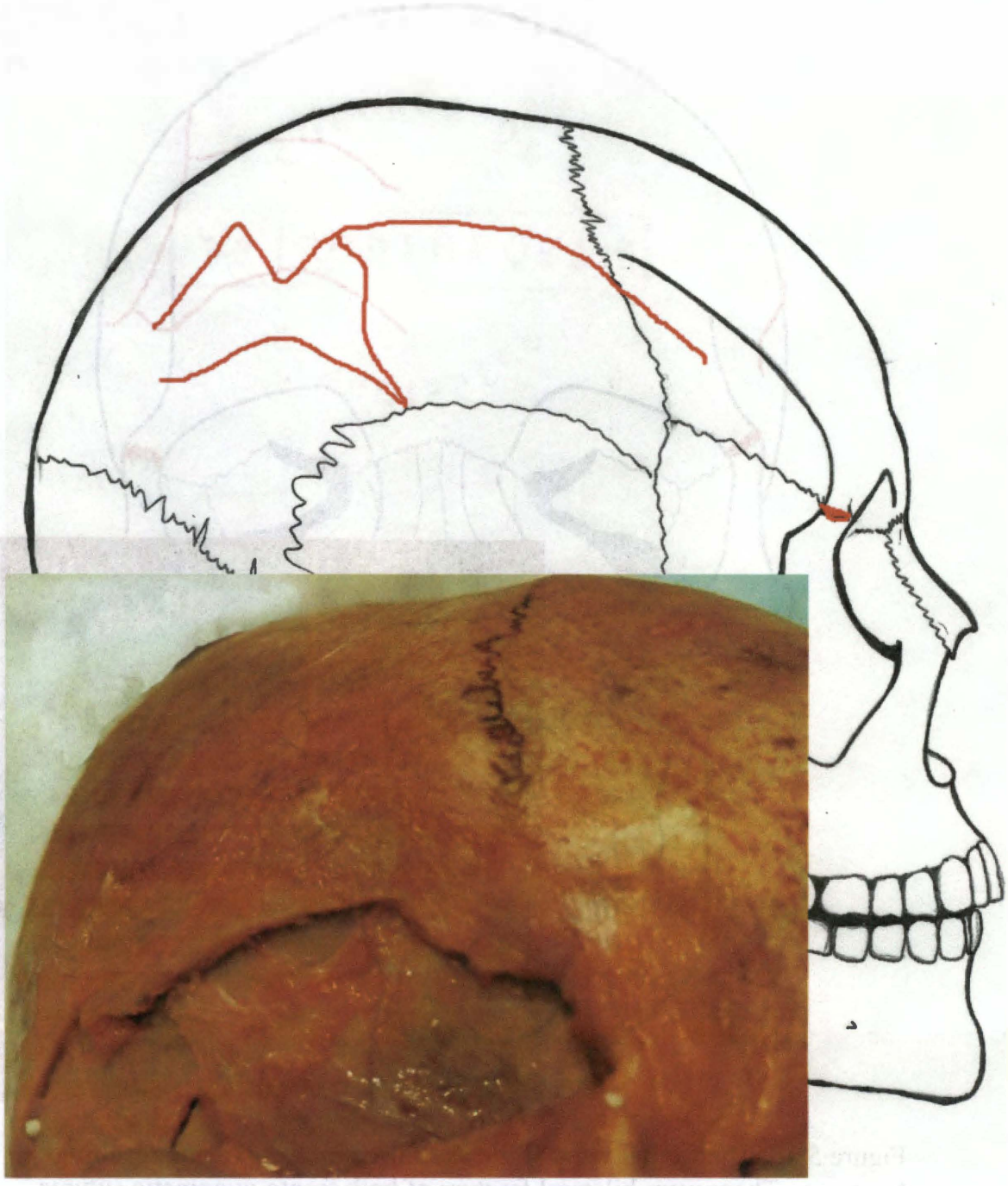

Figure 5.9 Right parietal, area on the opposite side from impact.

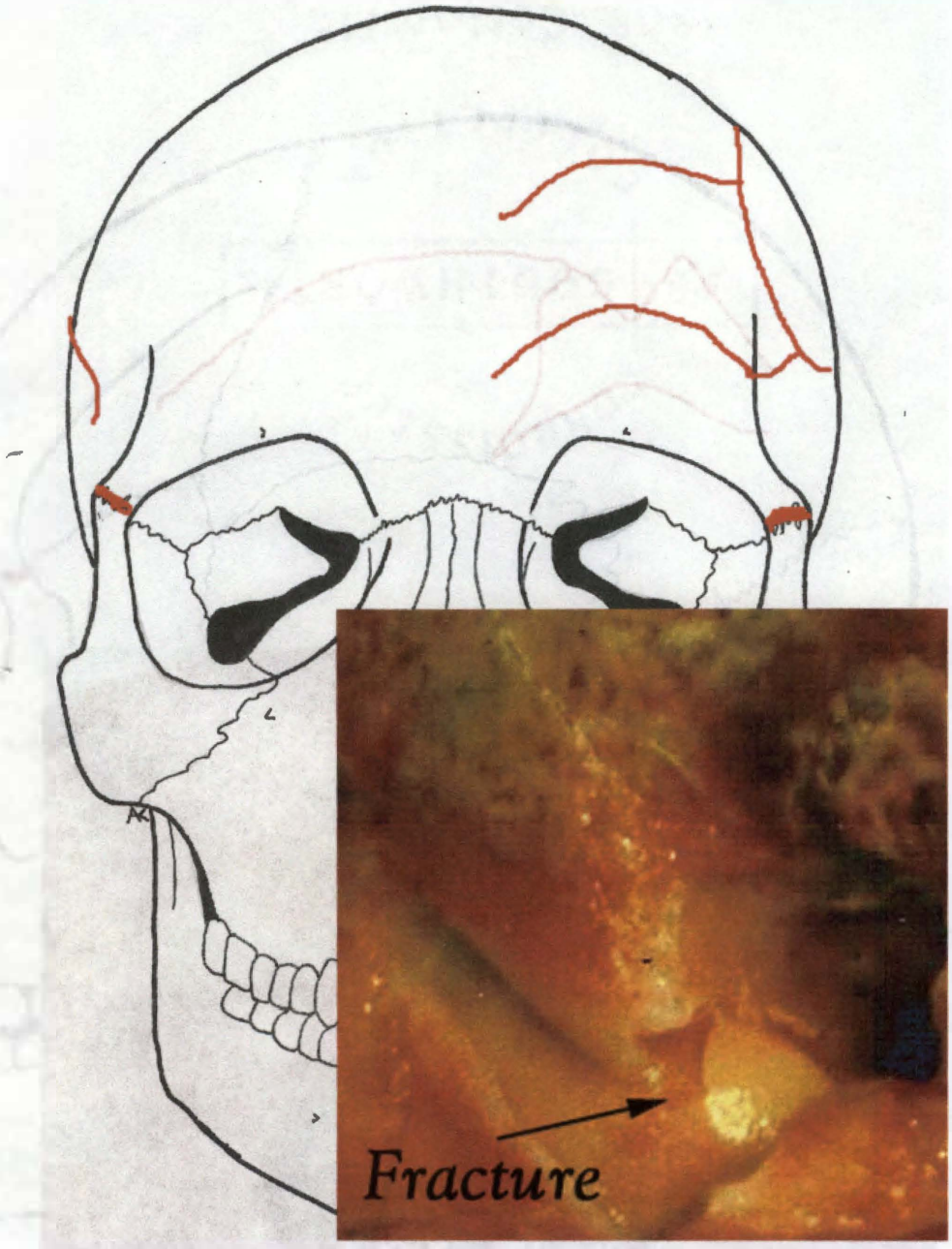

Figure 5.10 The frontal view of the skull used in test five and resulting fractures. There were bilateral fracture of both fronto-zygomatic sutures (insert).

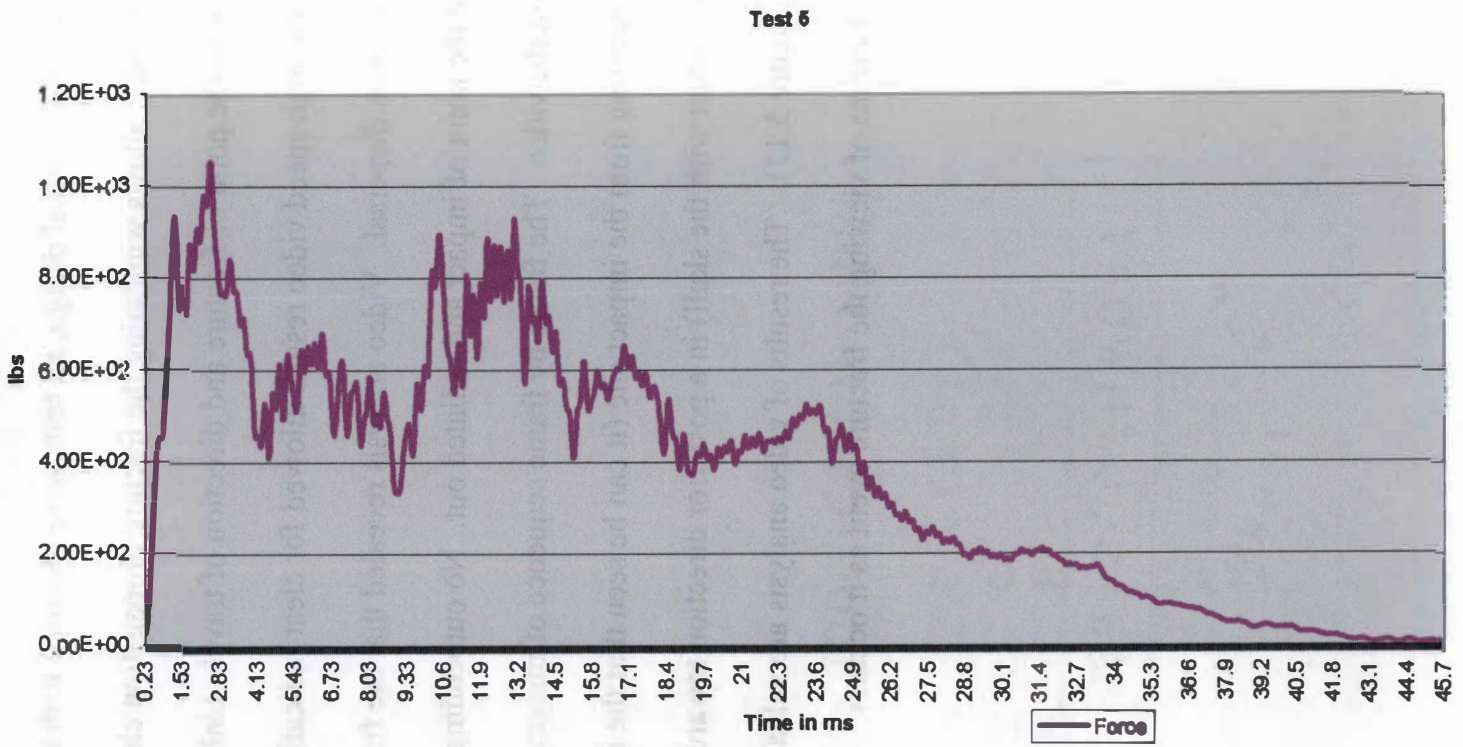

Figure 5.11 Force in pounds (recorded in scientific notation) to time in milliseconds for Test 5.

Results from high speed video

In the experimental design, all tests were recorded with high speed video. The video allows witnessing the fracture propagation clearly demonstrating the point of fracture and direction of travel. Unlike Gurdjian, the high speed video results allowed for clear indication of fracture direction dispersal. Video analysis revealed that the fractures initiated at the point of impact and radiated out. No outbending were observed in the video. The frame by frame sequence of images show fractures traveling from the impact site (it can be seen that the impactor is already in contact with the skull) in a posterior direction towards the occipital (Figure 5.12). The results of video analysis are valuable by providing a means of viewing the fracture event as it occurrs.

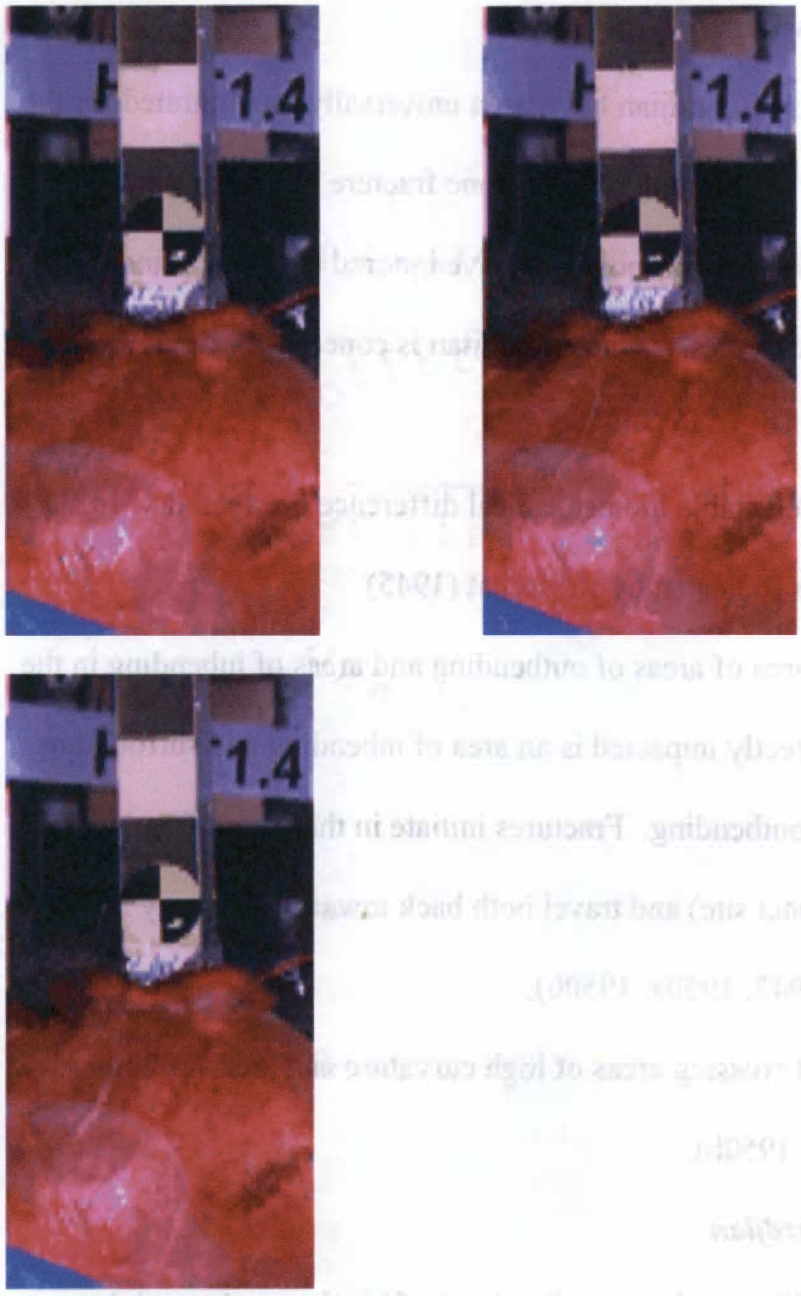

Figure 5.12 The line of fracture propagation (read left to right) in test five.

Chapter 6: Discussion

The findings of Gurdjian have been universally incorporated for the most part with out questioning into the bone fracture literature since their publication. As a rule, anthropologists have ignored the basic principle of science – rethink and retest – where Gurdjian is concerned. Review of Gurdjian reveals:

1. There was no detectable biomechanical difference between dry, fresh, and living skulls as indicated by stresscoat (1945).
2. Impact causes area of areas of outbending and areas of inbending in the skull. The area directly impacted is an area of inbending and surrounding areas are areas of outbending. Fractures initiate in the areas of outbending (remote to the impact site) and travel both back towards and away from the point of impact (1947, 1950a, 1950b).
3. Fractures avoid crossing areas of high curvature and areas of buttressing in the skull (1947, 1950b).

Problems with Gurdjian

While Gurdjian studies was far ahead of his time and certainly set a standard for the experimental study of fracture mechanics, they suffered from some inherent problems. These issues surfaced when it was noted that the predictions made from experimental models are not seen in real

case studies. An overwhelming amount of forensic evidence indicates that fractures in the skull initiate at the point of impact. In fact, the detailed fracture patterns that Gurdjian described for each area of the skull bear little resemblance to modern forensic cases.

One primary problem with Gurdjian is the use of stresscoat, a brittle lacquer, to serve as a proxy for human bone. In the 1945 article, when the stresscoat technique was tested Gurdjian states that the suture lines were a concern for fracture propagation. It is well known that sutures can act as energy "sink holes" causing termination of fractures (Symes et al, 1989). However, once the sealant and stresscoat were applied to the dried skull, Gurdjian notes that the sutures were no longer a problem. This indicates that the stresscoat technique has negated the presence of sutures, already compromising the biomechanical integrity of the skull.

Gurdjian also found no biomechanical difference between dry, fresh, and living skulls using stresscoat (1945). The changes that occur in bone through drying are drastic and well documented (Galloway 1999, Turner and Burr 1993). Fracture patterns change as moisture is lost as well the resistance to energy. In a later study, Gurdjian (1975) even noted this contrast calculating that it only took 10% of the energy to fracture a dry skull as a fresh one. The similarity between the stresscoat fractures in dry,

fresh, and living crania demonstrate that stresscoat is not a good proxy for human bone and does not adequately reflect the biomechanics of the skull. Pure brittle and elastic materials have different inherent biomechanical properties than bone, which is an intermediate material (Stock and Corderoy 1969).

While bone has a degree of elasticity, it is not as elastic as the Gurdjian theory predicts (Turner and Burr 1993). The considerable amount of outbending described by research is indicative of a material far more elastic than bone. The drastic degree of bending illustrated by DiMaio (2001) and Galloway (1999) and the tearing described by Berryman and Symes (1998) are more likely to describe a rubber ball impact rather than a human skull. Galloway (1999) even describes the human skull as a "semi-elastic ball." As a viscoelastic material, bone deformation is dependent on the rate of loading. At a rate of loading common to blunt force trauma, bone fails before inbending and outbending occurred (Keaveny and Hayes 1993). Gurdjian used this principle for his explanation that fractures initiate far from the point of impact and radiate back towards it.

The results from this study demonstrate that failure occurs first in the immediate area of impact with radiating fracture traveling from this point. No areas of drastic inbending or outbending were created. There was no

indication of fracture begining at any region other than the point of impact as proposed by Gurdjian (1950b), Di Maio (2001), and Galloway (1999). Fractures were documented as radiating from the point of impact and this propagation was captured on high speed video.

Gurdjian (1947) also theorized that fracture propagation is affected by the curvature of the cranium. The results from this study agree with this theory with most radiating fractures following the plane of least curvature in the cranium. Impact to the parietals produced fractures that radiated either distally to the sqaumosal suture, or in a dorsal/ventral direction. Few fractures were seen to radiate superiorally towards the sagittal suture, a region of curvature.

One skull was tested with a semi-rigid boundary to see if that would affect the biomechanics and replicate the Gurdjian theory. The results included drastic differences in fracture patterning, but no fractures were initiated at any remote locations.

The results of this study refute Gurdjian's notion that fracture initiation begins at a location remote to the point of impact. All fractures, regardless of the constraint of the cranium radiated out from the impact site. This should be fully taken into consideration by anthropologists when conducting fracture pattern analysis and trauma interpretation. The

explanation that a fracture is a result of a blow to an unassociated area is no longer acceptable.

References

Alms M. 1961. Fracture mechanics. The Journal of Bone and Joint Surgery 438: 162-166.

Antich PP. 1993. Ultrasound study of bone *in vitro.* Calcified Tissue International 53(Suppl 1): S157-S161.

Ashman RB, Cowin SC, VanBuskirk WC, Rice JC. 1984. A continuous wave technique for the measurement of the elastic properties of cortical bone. Journal of Biomechanics. 17: 349-361.

Berryman HE, Symes SA. 1998. Recognizing gunshot and blunt cranial trauma through fracture interpretation. In: Reichs KJ, editor. Forensic Osteology: Advances in the identification of human remains. Illinois: Charles C. Thomas.

Berryman HE, Symes SA, Smith OC, and Moore SJ. 1991. Bone fracture II: gross examination of fractures. Paper presented to the 43rd Annual Meeting of the American Academy of Forensic Sciences, Anaheim California.

Bonfield W, Behiri JC, and Charalambides C. 1985. Orientation and age releated dependence of the fracture toughness of cortical bone. Biomechanics; current interdisciplinary research; selected proceedings of the Fourth Meeting of the European Society of Biomechanics, 185-188.

Bonfield W and Li CH. 1965. Deformation and fracture of bone. Journal of Applied Physics 37: 869-875.

Bouvier M. The biology and composition of bone. In: Cowin SC, editor. Bone Mechanics. Boca Raton: CRC Press. p 1-14.

Brinckmann P, Frobin W, and Leivseth G. 2002. Musculoskeletal biomechanics. New York: Thieme.

Chapon A. 1984. Experimental models in biomechanics of impact. In: Aldman B and Chapon A, editors. The Biomechanics of Impact Trauma. Amsterdam: Elsivier Science.

Cowin SC. 1989. Mechanics of materials. In: Cowin SC, editor. Bone Mechanics. Boca Raton: CRC Press. p 15-42.

DiMaio VJ and DiMaio D. 2001. Forensic pathology. Second Edition. CRC Press.

Evans FG. 1970. Biochemical implications of anatomy. In: Cooper JM, editor. Selected topics on biomechanics: proceedings of the C.I.C symposium on biomechanics. Indiana University.

Evans FG. 1973. Mechanical properties of bone. Springfield, IL: Charles C. Thomas.

Frost HM. 1967. An Introduction to Biomechanics. Springfield, IL: Charles C. Thomas.

Galloway A. 1999. Fracture patterns and skeletal morphology: introduction and the skull. In Galloway A, editor. Broken Bones. Springfeild, IL: Charles C. Thomas.

Gonza ER. 1982. Biomechanics of long bone injury. In: Biomechanics of Trauma. Baltimore: Williams and Wilkins. p 1-24.

Gurdjian ES. 1975. Impact head injury, mechanism, clinical and preventive correlations. Springfeild, IL: Charles C. Thomas.

Gurdjian ES, and Lissner HR. 1945. Deformation of the skull in head injury: a study with the "stresscoat" technique. Surgery, Gynecology, and Obstetrics 81:679-687.

Gurdjian ES, Lissner HR, and Webster JE. 1947. The mechanism of production of linear skull fractures. Surgery,Gynecology, and Obstetrics 85:195-210.

Gurdjian ES, Webster JE, and Lissner HR. 1949. Studies on skull fracture with particular reference to engineering factors. American Journal of Surgery 78: 736-742.

Gurdjian ES, Webster JE, and Lissner HR. 1950a. The mechanism of skull fracture. Journal of Neurosurgery 106-114.

Gurdjian ES, Webster JE, and Lissner HR. 1950b. The mechanism of skull fracture. Radiology 54:313-338.

Gurdjian ES, Webster JE, and Lissner HR. 1953. Observations on prediction of fracture site in head injury. Radiology 60:226-235.

Harkess JW, Ramsey WC and Ahmadi B. 1984. Principles of fracture and dislocations In: Rockwood CA and Green DP, editors. Fractures in adults, Volume 1. Philadelphia, PA.

Hein PM, Schulz E. 1990. Contrecoup fractures of the anterior cranial fossa as a consequence of blunt force caused by a fall. Acta Neurochir 105: 24-29

Hodgson VR, Brinn J, Thomas LM, and Greenberg SW. 1970. Fracture behavior of the skull frontal bone against cylindrical surfaces. In: Proceedings of Fourteenth Stapp Car Crash Conference. Ann Arbor Michigan. p 341-355.

Johnson E. Current developments in bone technology. In: Schiffer MB, editor. Advances in Archaeological Method and Theory, vol 8. Orlando: Academic Press.

Keaveny TM, and Hayes WC. 1993. Mechanical properties of cortical and trabecular bone. In: Hall BK, editor. Bone Vol. 7. Boca Raton: CRC Press. p 285-344.

Ketlinski R. 1970. Can high speed photography be used as a tool in biomechanics? In: Cooper JM, editor. Selected topics on biomechanics: proceedings of the C.I.C symposium on biomechanics. Indiana University.

Knight B. 1996. Forensic Pathology, Second edition. London: Arnold.

LeCount ER, and Apfelbach CW. 1920. Pathological anatomy of traumatic fractures of cranial bones. Journal of American Medical Association 74(8): 501-511.

Low J, and Reed A. 1996. Basic biomechanics explained. Oxford: Butterworth-Heinmann Ltd.

McElhaney JE, Reynolds VL, Hilyard JF. 1976. Handbook of human tolerance. Tokyo: Japanese Automobile Research Insititute.

Melvin JW. 1993. Fracture mechanics of bone. Journal of Biomechanical Engineering. 115:549-554.

Moritz AR. 1954. The pathology of trauma. Philidelphia: Lea and Febiger.

Nordin M, and Frankel VH. 1980. Biomechanics of whole bone and bone tissue. In: Frankel VH and Nordin A, editors. Basic Biomechanics of the Skeletal System. Philadelphia. p 15-60.

Oxnard CE. 1993. Bones and bones, architechure and stress, fossils and osteoporosis. Journal of Biomechanics 26: 63-79.

Piekarski K. 1970. Fracture of bone. Journal of Applied Physics 41: 215-223.

Reilly DT, and Burnstein AH. 1974. The mechanical properties of cortical bone. Journal of bone and joint surgery. 56:1001-1022.

Roark RJ , and Young WC. 1975. Formulas for stress and strain. New York: McGraw Hill.

Stock TAC, Corderoy DJH. 1969. In: Osbore CJ, Gifkins RC, Hoggart JS, Mansell DS, editors. Fracture. Austriala: Butterworth and Company. p 69-79.

Symes SA, Berryman HE, and Smith OC. 1989. The changing role of the forensic anthropologist: pattern and mechanism of fracture production. Lecture presented at Mountain, Swamp, and Beach meeting of practicing forensic anthropologists. Gatlinburg, TN.

Turner CH, and Burr DB. 1993. Basic biomechanical measurements of bone: a tutorial. Bone 14: 595-608.

Yoganandan N, Pintar FA, Sances A, Walsh PR, Ewing CL, Thomas DJ, Snyder RG. 1995. Biomechanics of skull fracture. Journal of Neurotrauma 12: 659-668.

Vita

Anne Meredith Kroman was born on May 11th, 1980 in Houston TX. After living in Texas, North Carolina, Missouri, and Kansas, she attended undergraduate at the University of Kansas. Anne was a University of Kansas merit scholar, and graduated with honors in three years with a BA in Anthropology. During her time at the University of Kansas, Anne became involved with on going bone trauma research at the Regional Forensic Center, in Memphis Tennessee. She moved to Knoxville, Tennessee in 2001 as a Masters student in Physical Anthropology. Anne is currently a PhD student in Physical Anthropology at the University of Tennessee, Knoxville.